Title

Metal complex strategies for photo-uncaging the small molecule bioregulators nitric oxide and carbon monoxide

Author

Ford, Peter C

Publication Date

2018-12-01

DOI

10.1016/j.ccr.2018.07.018

Peer reviewed

Metal complex strategies for photo-uncaging the small molecule bioregulators nitric oxide and carbon monoxide

Peter C. Ford*
Department of Chemistry and Biochemistry, University of California, Santa Barbara;
Santa Barbara, CA. 93106-9510 USA
Email: ford@chem.ucsb.edu

Abstract:

Photochemical release (uncaging) of small molecule bioregulators (SMBs) such as nitric oxide (NO) or carbon monoxide (CO) at physiological sites offers exquisite control of timing, location and dosage. However, photo-uncaging faces two major problems that challenge its therapeutic applications: the relatively poor transmision of visible light through tissue and the need to deliver the appropriate precursors to the desired targets. In this brief review are discussed research activitites that address these issues of spatial-temporal control.

Contents:

Keywords: nitric oxide; carbon monoxide; photo-uncaging; photoCORM; PhotoNORM; two-photon excitation; quantum dots; upconverting nanoparticles; nanomaterials; macrophage.

*Corresponding author Email: ford@chem.ucsb.edu

1. Introduction:

This review discusses innovative strategies for the photochemical release (uncaging) of the small molecule bioregulators nitric oxide (NO, aka nitrogen monoxide) and carbon monoxide (CO) at specific physiological sites. Localized delivery of these moieties is of interest for potential therapeutic applications. Key concerns include the roles of NO in the cardiovascular system, in antibacterial applications and in cancer therapy [1-4] as well as the roles of CO in suppressing inflammation, wound healing and anti-bacterial activity [5-7]. Precise spatial-temporal control is essential, since, for example, NO delivered systemically can induce precipitous blood pressure decline; indeed, this is a cause of toxic shock. Dosage control is also important, since high levels of NO can kill tissue by inducing cell apoptosis, but low levels may instead be proliferative [8,9].

The revolutionary discoveries in the late 1980's that nitric oxide is synthesized endogenously and that such a simple molecule plays a plethora of roles in mammalian physiology led to the remarkable outpouring of research relevant to the chemical biology and biomedicine of NO. A key issue that emerged was what techniques could be used to deliver exogenous NO to specific targets. As a result, a number of compounds capable of the thermal release of NO were developed [10]. The story of carbon monoxide as a small molecule bioregulator (SMB) is similar. Although it has been known for decades that CO is generated endogenously by constitutive and inducible forms of the enzyme heme oxygenase [11], its bioregulatory and potentially therapeutic aspects were only more recently recognized. Several compounds called CORMs (CO releasing moieties) have been developed that are effective for the thermochemical CO release at physiological targets [6,12]. Interestingly, most of these CORMs are transition metal carbonyls, the ruthenium complex $Ru(CO)_3(gly)Cl$ (CORM-3, gly^- = glycinato) being an example [13]. The foci of the present discussion are photochemical methodologies for the targeted release of these small molecule bioregulators (SMBs).

If the SMB in the form of a photochemical precursor is benign, it is defined as "caged". Electronic excitation releases or transforms it into an active or "uncaged" form. The external signal (light) determines the location and timing of SMB release, while the quantity of light absorbed controls the extent of photoreaction (i.e. dosage). Thus, photo-uncaging defines the *location*, *timing* and *dosage* of SMB delivery and has value both as an investigative tool and in the potential therapy of specific disease states [14-16]. An example of a therapeutic application would be the uncaging of a radiation sensitizer during radiotherapy. Hypoxic regions of malignant tumors are more γ-radiation resistant than are normoxic tissue; therefore, one could reduce the collateral damage from such treatments by increasing the sensitivity of the targeted site [17]. NO is both a radiation sensitizer [18] and an exceptionally potent vasodilator [1,19], so releasing even nanomolar concentrations of NO at a targeted site synchronously with γ-radiation treatment [20] would enhance the efficacy of radiotherapy [21].

Developing such applications requires elucidating the fundamental photochemistry and photophysics of effective SMB precursors as well as defining the mechanisms for transporting these species to the physiological sites of interest. The photo-uncaging of NO has been an active research topic in this laboratory [20,22-33] and others [34-43] for several decades, while the photo-uncaging of CO has drawn growing attention for the past decade [44-54]. These two topics were the subject of a several comprehensive reviews over the past several years [5, 55], so the

present article will not duplicate those efforts. Instead, we focus on presenting an overview of different photo-uncaging strategies for these two SMBs with an emphasis on studies from this laboratory, but also drawing attention to newer reports from other researchers. We will use the term "photoCORM" (photo-activated CO releasing moiety), which we coined several years ago for caged carbon monoxide [44], and for consistency the parallel term "photoNORM" (photo-activated NO releasing moiety) for caged nitric oxide [55a].

2. Key Issues in photo-uncaging

Notably, different bioregulatory tasks require different net or steady state quantities of SMB release. Since small molecules can defuse away from a targeted site and/or are consumed by various physiological processes, the rate of the photo-uncaging process is of critical importance. This rate is defined for single photon excitation by the product of the quantum yield (Φ_i) for the photoreaction of interest times the intensity of light absorbed (I_{abs}) by the photochemical precursor (eq. 1),

$$R_i = \Phi_i \, x \, I_{abs} \qquad (1)$$

where R_i is the rate of the particular photochemical process of interest and Φ_I is the efficiency by which excited states once formed decay along that specific pathway. (Φ_I is unit-less.) I_{abs} is a function both of the incident light intensity I_i and of the absorbance Abs(λ) by the photochemical precursor at the irradiation wavelength(s) λ_{irr}. (See the Appendix where the relationship between I_{abs} and photochemical rates are discussed in greater detail). Thus, one approach to enhancing uncaging rates is to increase the molecular absorbance by designing conjugate systems with strongly absorbing antennas (Scheme 1). However, it is important to recognize that such an antenna will only work as a photosensitizer if there are acceptor states at appropriate energies on the photochemical CO precursor.

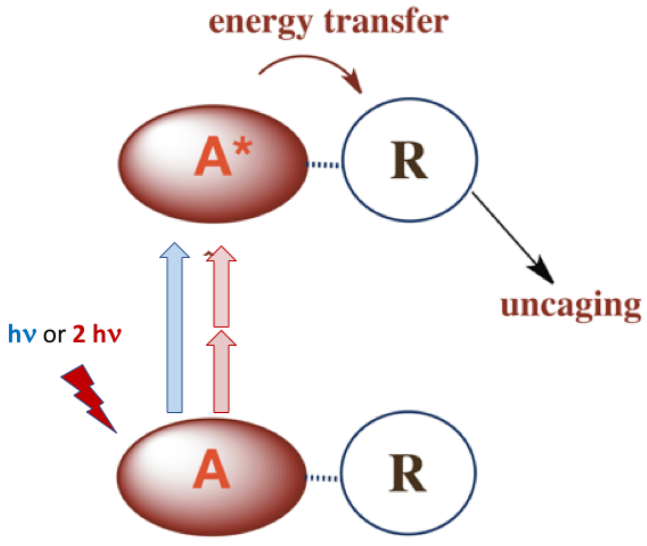

Scheme 1. A is the antenna, **R** is a precursor of a SMB that is uncaged once **R** is photosensitized by one- or two-photon excitation.

Another important issue that must be addressed when considering photochemically activated therapies is the wavelength of the excitation light. Photochemical reactivity is not sufficient for *in vivo* uncaging. Any biomedical application, other than subcutaneous, needs to be responsive to the λ_{irr} where light penetration through tissue is optimal. Such penetration is shallow for UV light and may be accompanied by collateral tissue damage. Transmission through tissue improves for longer visible wavelengths and is optimal for NIR wavelengths [56]. One can address this issue by modifying the optical properties of the corresponding photoNORMs and photoCORMs to shift the effective excitation wavelengths to lower energy. We have also approached this problem by developing molecular conjugates that can harvest *multiple* NIR photons to access the higher energy reactive states needed to effect the desired uncaging.

As noted above, photo-uncaging provides greater spatial-temporal control of SMB release. Nonetheless, it is clear that it would be more effective (and probably safer) to target the delivery of the caged compound to the organ or tissue of interest rather than overwhelming the host by flooding the system. So, targeting is an important consideration in the design of new compounds or conjugates to be used in this manner. There are a number of strategies that might be effective. Physical targeting may be achieved by using an implant and/or injection while biological targeting might be achieved by using antibodies or proteins that seek out specific tissue types. Another biological strategy would be to recruit immune cells, such as macrophages, loaded with a photochemical precursor of the desired SMB and to use this mechanism to target sites of inflammation such as tumors or wounds.

The work describe in this article is largely concerned with issues relevant to photo-uncaging SMBs from coordination compounds.[1] Our approach focuses on two goals: (a) designing complex conjugate systems that utilize deep tissue penetrating near-infrared (NIR) light as the excitation source and (b) developing carriers for the conjugates that effectively target desired sites. Although we have directed our attention to NO and CO, *these strategies should be applicable to the uncaging of any bioactive small molecule*.

3. Nitric oxide and carbon monoxide precursors.

There are a number of common issues to consider when developing an effective photoNORM or photoCORM or a photochemical precursor of any other SMB for therapeutic applications. One would be solubility in aqueous solution or at least in a medium such as aqueous DMSO often used for drug delivery, although as we will see below, the use of vesicles or polymer carriers may alleviate that requirement. Another would be reasonable stability in aerated aqueous media at physiological temperatures and other conditions typical to living organisms. While the expectation for thermally activated NO or CO precursors would be spontaneous decay

[1] It should be noted that alternative approaches to photo-uncaging of NO and CO based on organic precursors are also under investigation by various researchers. For example, nitroaromatics Ar-NO_2 when irradiated undergo photoisomerization to the nitrito analog Ar-ONO followed by cleavage of the ArO-NO bond to give NO plus the phenoxy type radical ArO• (see ref. 37d, a recent review that discusses applications of such photochemical NO precursors in detail). Similarly, 3-hydroxyflavone derivatives have been shown to eject CO when irradiated with shorter visible wavelengths (see references 52ab)

at known rates, a photoNORM or photoCORM should be non-toxic and relatively stable and should release its payload only when triggered externally with light. Another is that the metal containing product after payload release should not have deleterious properties, such as unwanted acute or long-term toxicity. Thus, it is important to characterize and identify such products and any secondary products formed by subsequent reactions under the conditions and to ascertain whether the observed physiological effects are due to SMB release or to other such products. Complexes of lighter metals that are more easily excreted might be preferable in terms of avoiding long-term toxicity. Lastly, as noted above, photoactivity at wavelengths relevant to the task is needed.

For the promiscuous SMB nitric oxide, the biomedical rationale for controlled delivery include NO's potent cardiovascular and antibacterial properties as well as potential roles in cancer therapy. For example, the use of NO to directly kill tumor cells has been a major focus of several laboratories, but one should proceed with caution in this case. As noted above, high localized levels of NO (>800 nm) can induce nitrosative stress and cell apoptosis, but lower levels of NO may instead induce tumor growth by stimulating angiogenesis [8,9]. For this reason, our approach draws from the view that NO delivery should be synergistic with other forms of treatment, such as chemotherapy [4,57] or radio-therapy [19-20]. NO is a radiation sensitizer, and we confirmed this in very early studies by using the Roussin's red salt $Na_2[Fe_2S_2(NO)_4]$ (RRS) as a photoNORM to deliver NO to hypoxic V79 cell cultures that thus displayed markedly enhanced sensitivity to γ-radiation [20]. Furthermore, in a living animal, the release of the potent vasodilator NO, even at nanomolar concentrations, should increase the localized tissue oxygenation [19] and thus may indirectly enhance the radiation killing of tumor tissue.

Another important feature of NO photo-uncaging is that, while NO diffuses fairly readily in biological media, it is also readily consumed by a variety of mechanisms, including oxidation to nitrite and nitrate [58]. As a result, its lifetime is relatively short (seconds) and the effects of NO photo-uncaging are localized.

With regard to carbon monoxide, the most likely targets are metal (largely heme) centers, where CO coordination may affect cell-signaling enzymes such as transcription factors, ion channels and O_2 transport and inhibit key processes such as the redox chain in mitochondria [5a]. For these cases, one might use dissociation constants for CO binding to the specific proteins (for example, 300 - 1000 nM for globins [59]) as an estimate for the localized CO concentrations necessary to have significant impact.

When faced with number of published and emerging photoNORMs and photoCORMs, one might ask: which of these and which method of delivery might have the most desirable properties? This is a difficult question to answer, since one must consider the task for which of these are being proposed. Once the task is identified, for example, treatment of a certain type of cancer, systematic comparison requires standardized tests to which each compound or conjugate and/or delivery method would be subjected, preferably by an independent laboratory. There are a number of issues that need to be considered including acute and long-term toxicity, specificity for the tissue targeted, and functional photochemical efficiency, among others.

3.1 ***PhotoNORMs:*** Since initiating studies of NO photo-uncaging in the 1990's, we have used theoretical, synthetic and mechanistic tools to develop and characterize a variety of

photoNORMs. The goal has been to lay the fundamental groundwork for systems that can find applications in mammalian physiology. There is a rich history of metal nitrosyl photochemistry, especially that involving metalloporphyrins [22]. Our more recent focus has been directed toward conjugate systems that can be triggered with the longer visible or NIR excitation wavelengths (λ_{irr}) that are more effective at transmission through mammalian tissue. Three such platforms are depicted in Figure 1: Cr(III) nitrito complexes, for example, *trans*-Cr(cyclam)$(ONO)_2^+$ ("CrONO", cyclam = 1,4,8,11-tetraza-cyclotetradecane), ruthenium nitrosyls such as the salen complex depicted, and iron-sulfur-nitrosyl clusters like the Roussin's red salt anion (**RRS**). PhotoNORMs based on each platform were shown to be stable under physiological conditions, and to release NO readily upon visible light photolysis. We have also collaborated with Prof. Yutaka Hitomi of Doshisha University (Kyoto, Japan) who developed a manganese complex $[Mn(NO)dpaq^{NO2}]BPh_4$ ($dpaq^{NO2}$ = 2-[*N*,*N*-bis(pyridin-2-ylmethyl)]-amino-*N*'-5-nitro-quinolin-8-yl-acetamido) [54b] that undergoes the photorelease of NO under excitation with very long visible irradiation wavelengths. Other ruthenium [34, 36, 40] and manganese platforms [54] have received attention in this field and represent some very creative synthesis efforts to design compounds that are photoactive at longer visible wavelengths [55a].

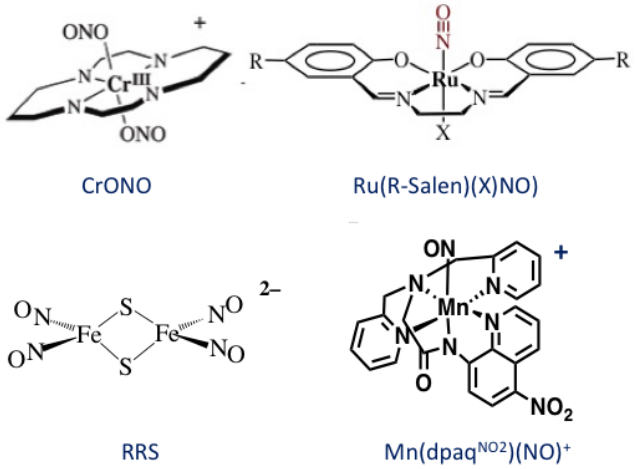

Figure 1. Examples of photoNORMs.

CrONO would appear to be an ideal photoNORM. It is stable in 37 °C aqueous buffer, it exhibits no acute toxicity in cell-culture experiments, and it displays high quantum yields for NO release (Φ_{NO}) at all λ_{irr} (365-546 nm) investigated [28b]. Flash photolysis experiments indicate that this occurs via reversible homolysis of a CrO-NO bond (Eq. 1) [28a]. As a result, net release of NO depends on trapping the Cr(IV) reactive intermediate by an oxidant such as O_2 or a reductant such as glutathione (GSH). Thus, CrONO is effective toward NO photo-uncaging in both oxidizing *and* reducing media. Myography studies with porcine aorta demonstrate cardiovascular relaxation resulting from NO release when CrONO is irradiated but no activity from the other chromium containing products.

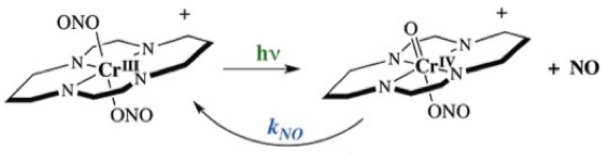

(1)

Our photosensitization experiments and TD-DFT computations [28b] point to the reaction occurring from the spectrally silent, doublet metal centered, ligand field state of the Cr(III) center presumably populated by rapid intersystem crossing from states formed by excitation of quartet-to-quartet, metal-centered (d-d) bands in the CrONO visible spectrum. However, these spin-allowed transitions are Laporte forbidden and have low molar extinction coefficients. Thus, the rate of photochemical NO generation R_{NO} (which equals Φ_{NO} x I_{abs}) is inherently slow owing to the low value of I_{abs} unless the localized concentration of CrONO is high. This feature led us to explore various antennas with much stronger absorption cross-sections to increase light collection efficiency and to accelerate the R_{NO} values by increasing I_a. Early examples from our laboratory demonstrated this principle with pendant aromatic chromophores as antenna for CrONO [60] and for Roussin's red salt [61-63] (Figure 2). Excitation of these chromophores was followed by energy transfer to the attached photoNORM leading to significantly enhanced rates of NO release from the antenna-free photoNORM under analogous conditions and incident excitation intensities I_i owing to higher absorbance (Abs) at that λ_{irr} and the relationship $I_{abs} = I_i(1-10^{-Abs(\lambda)})$. Notably, the fluorescence from each of these pendant chromophores is not fully quenched by the attached photoNORM, and thus provides a tool for tracking the location of these species [63].

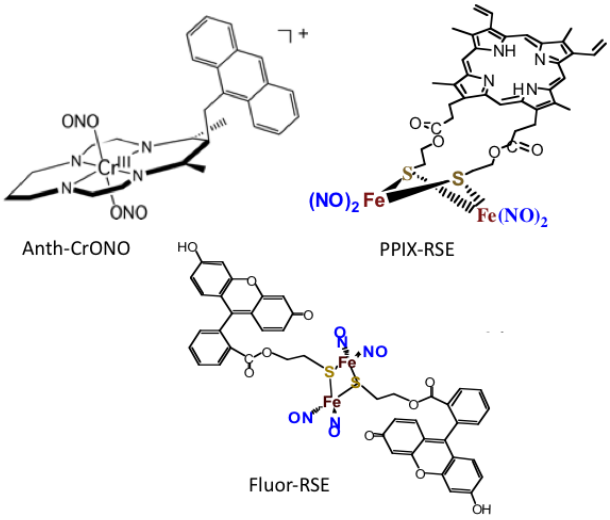

Figure 2. Pendant chromophores on photoNORMs (Anth = anthracene; PPIX = protoporphyrin-IX; Fluor = fluorescein; RSE = red salt ester)

***3.2 PhotoCORMs*.** The mechanisms of CO release from metal carbonyls (eq. 2) has long been the subject of photochemical studies [64]. However, much of the interest lay in the organometallic and catalysis relevant chemistry of these compounds and the photolysis generated intermediates [65]. As a consequence, most such investigations were carried out in anaerobic and anhydrous media, neither condition being very compatible for possible

therapeutic applications. Although there were earlier studies where CO was delivered to biological targets via the "cold light" photolysis of the simple metal carbonyl $Mn_2(CO)_{10}$ [66], Schatzschneider and coworkers can be credited with being the first to design metal carbonyl complexes for this purpose [49a]. Those researchers used dimethyl sulfoxide (DMSO) solutions to deliver the complex salt *fac*-$[Mn(CO)_3(tpm)]PF_6$ (tpm = tris(pyrazolyl)methane) directly to HT29 colon cancer cells where CO release was triggered by 365 nm light, resulting in significant photoinduced toxicity. This observation raises an interesting question about the goals of CO delivery that parallel some of the issues that plague NO delivery. If the goal is to promote wound healing as has been argued as an important property of exogenously applied CO [6], this would imply CO enhanced cell growth and motility. If the goal is anti-tumor or anti-bacterial activity, then cell toxicity is desired. The Janus character of these two SMBs makes controlling the timing, location and dosage of the delivery options all the more important.

$$ML_x(CO)_y \xrightarrow{h\nu} ML_x(CO)_{y-1} + CO \qquad (2)$$

Shortly after the Schatzschneider report, Dale Rimmer of this laboratory [44] completed a quantitative study of the water-soluble tungsten carbonyl complex $Na_3[W(CO)_5(TPPTS)]$ ($TPPTS^{3-}$ is the tris(sulfonato-phenyl)phosphine trianion), which also was photoactive at near-UV wavelengths. Aqueous, aerobic buffer solutions of this photoCORM undergo photo-induced loss of one CO with a high quantum yield (Φ_{CO} = 0.90 and 0.6 for λ_{irr} = 313 and 405 nm, respectively) followed by subsequent slow oxidation of the $W(CO)_4(H_2O)(TPPTS)^{3-}$ photoproduct to release one to two additional CO's (eq. 3). In this report, Rimmer et al also described methodologies based on gas chromatography and on infrared spectroscopy for quantitatively measuring the amount of CO released under these conditions as alternative to the commonly used myoglobin assay [67].[2]

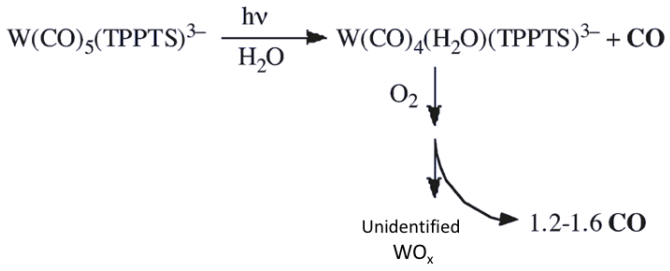

(3)

Neither of these photoCORMs are photoactive at longer range visible or NIR wavelengths, so any potential therapeutic value would be restricted to surface applications. For this reason, there has been considerable effort at extending this type of photoactivity to longer wavelengths [45,51-53,55] (Figure 3). To do so, one has to be attentive to the nature of the excited states that might lead to CO dissociation. We will take for example the group 6 M(0) complexes (M = Cr, Mo, W) of the type $M(CO)_5L$ or $M(CO)_4(LL)$, where L is a monodentate ligand such as pyridine (py) or a phosphine (R_3P) and LL is a bidentate heterocycle such as 2,2'-bipyridine (bpy) or 1,10-

[2] The commonly used method for demonstrating CO release from various CORMs and photoCORMS involves trapping the CO with deoxymyoglobin and measuring changes in the optical spectrum (ref 67). While this method is sensitive, it is not effective in aerobic media. More recently fluorescent probes for CO have been developed [55].

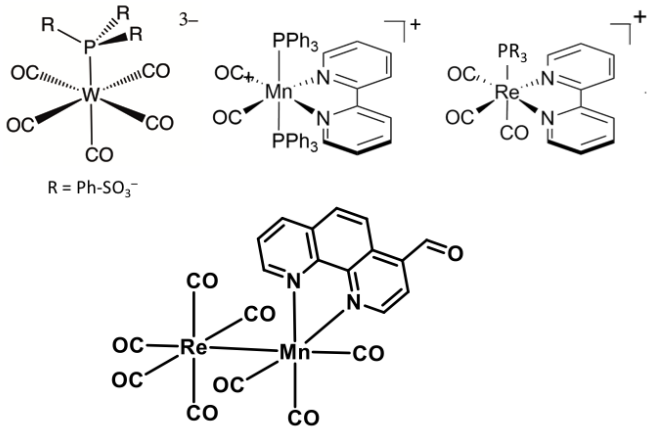

Figure 3. Some photoCORM examples.

phenanthroline (phen) (Figure 3). The same arguments apply to the group 7 M(I) complexes (M = Mn or Re) such as *fac*-$M(CO)_3(LL)X$ or fac-$M(CO)_3(LL)(L)^+$, the photochemistry of which have been the subject of numerous reports. The electronic transitions that dominate the lower energy spectra of these compounds are ligand field (LF or d–d) and metal-to-ligand charge transfer (MLCT) in character [64]. The metal-centered LF excited states of these low spin d^6 complexes involve promoting electron density from π-bonding orbitals to σ-antibonding orbitals with respect to these M-CO bonds. Thus, it is not surprising that excitation of d–d bands leads to ligand photodissociation with high quantum yields from LF excited states. However, carbonyls are strong field ligands, therefore, direct excitation of LF bands in metal carbonyls tend to occur at fairly high energies (UV or near-UV wavelengths). The MLCT bands have high extinction coefficients and can be tuned by electron withdrawing substituents to give strong visible absorptions. Since MLCT excitation promotes electron density from M-CO π^b orbital(s) to ligand π^*-orbital(s), it is much less obvious that the resulting MLCT excited state will be strongly labilized toward CO dissociation.

For example, Wrighton et al [68] long ago demonstrated with a series of $W(CO)_5(py\text{-}Y)$ complexes that tuning the MLCT excited state to energies substantially lower than the LF state excited state led to markedly less efficient ligand labilization as shown previously with analogous ruthenium complexes. While the MLCT excited states may be susceptible to an associative ligand substitution mechanism in a coordinating solvent [69] owing to the diminished electron density at the metal, the efficiency of CO labilization is likely to be significantly diminished. Indeed, much of the photoactivity attributed to excitation into such MLCT states may be the result of thermal back population into the higher energy, more reactive LF excited states. From a practical perspective, one may not care about the mechanism, so long as the desired CO labilization at longer wavelength is accomplished, but understanding these pathways would allow a more systematic approach to the desired outcome.

There various ways to address this conundrum. For example, for homologous W and Cr complexes or homologous Re and Mn complexes, the lighter element will express the lower LF excited state energies and should be more labile toward photodissociation at longer excitation wavelengths. Thus, while several fac-$Re(CO)_3(LL)(L')$ complexes have demonstrated the attractive features as being both luminescent and photoactive toward CO dissociation [48, 51a, 70], none

of these show labilization at longer visible λ_{irr}. For those complexes that are also luminescent, Wilson and coworkers have noted some quenching by O_2, raising the possibility that these might have bimodal action as CO and singlet oxygen generators [48]. For the Mn(I) analogs with weaker ligand field splitting, there are now numerous examples of CO labilization at visible λ_{irr} [51c, 55, 71] but pushing these excitation wavelengths far into the red remains a challenge.

Zhi Li and coworkers from this laboratory recently introduced a different strategy to address the question of CO labilization from stable metal carbonyls at longer visible and NIR λ_{irr} in aerobic media [47]. The dinuclear rhenium-manganese carbonyl complexes $(CO)_5ReMn(CO)_3(LL)$ (LL = phen (**1**), bpy (**2**), biquinoline (biq, **3**) or phenanthroline-carboxaldehyde (phen-CHO, **4**)) each display a strong, metal-metal bond to ligand ($\sigma_{MM} \rightarrow \pi_L^*$) charge transfer (MMLCT) absorption band at longer wavelengths, tunable by modifying the bidentate heterocycle LL (Figure 4).

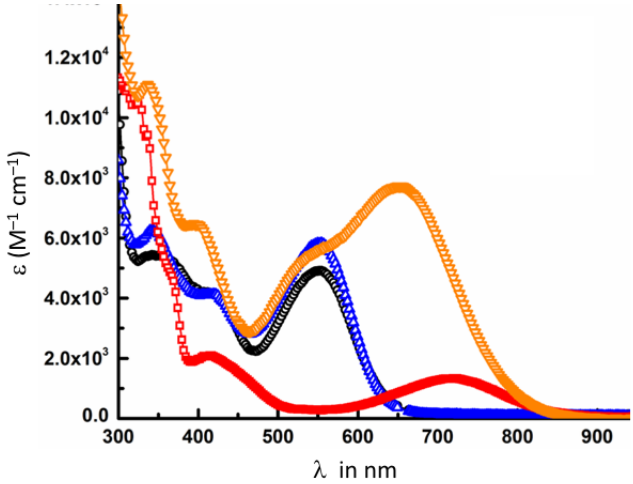

Figure 4. Absorption spectra of $(CO)_5ReMn(CO)_3(phen)$ (**1**, blue, λ_{max} = 550 nm), $(CO)_5ReMn(CO)_3(bpy)$ (**2**, black, 550 nm), $(CO)_5ReMn(CO)_3(biq)$ (**3**, red, 719 nm) and $(CO)_5ReMn(CO)_3(phen\text{-}CHO)$ (**4**, orange, 652 nm) in ambient temperature, aerobic ACN showing the strong MMLCT absorption bands. (Adapted from ref. 47)

Photolysis at red (659 nm, **1** or **2**) or NIR (794 nm), nm, **3** or **4**) λ_{irr} leads to reversible homolytic Re-Mn bond cleavage to give the corresponding mononuclear metal radicals (e.g., eq. 4) with quantum yields Φ_{MM} as large as 0.41 for **1**. In oxygenated media, these radicals are efficiently trapped by dioxygen to form intermediates labile toward CO release via secondary thermal and/or photochemical reactions as determined by gas chromatographic analysis. Exhaustive photolysis of **1** at 659 nm released two equivalents of CO, while no CO release was detected in deoxygenated solutions.

$$(CO)_5Re\text{-}Mn(CO)_3(phen) \xleftarrow{h\nu} (CO)_5Re\cdot + \cdot Mn(CO)_3(phen) \qquad (4)$$

Complexes **1-4** provide proof-of-principle that long-wavelength MMLCT photoactivation of dinuclear complexes can trigger photochemical CO release in aerobic media, but they are not soluble in aqueous media. This hydrophobic character may be an advantage when used within a biocompatible polymer matrix or with amphiphilic polymer-based vesicles or nanocarriers as described below. Another option would be to modify the LL ligands to enhance aqueous

solubility. For example, conjugation of $(CO)_5ReMn(CO)_3$(phen-CHO), with an amine-terminated polyethylene glycol (PEG) oligomer (eq. 5) gives a water-soluble derivative with similar photochemistry. The absorption spectrum of this material displayed a broad band at ~ 569 nm, a shoulder at 700 nm and absorbance extending beyond 800 nm. NIR photolysis (794 nm) showed this material to be photoactive in aerobic, pH 7.4 solution, but Φ_{MM} proved to be quite modest ($\sim 10^{-3}$). Similar systems are the subjects of on-going studies in this laboratory.

$$(CO)_5ReMn(CO)_3(\text{phen-CHO}) + H_2N\text{-PEG} \longrightarrow (CO)_5ReMn(CO)_3(\text{phen-CHNPEG}) + H_2O \qquad (5)$$

A related approach by Askes et al [53a] used red light (635 nm) excitation of palladium(II) tetraphenyl-tetrabenzoporphyrin Pd(TPTBP) to photosensitize decomposition of the manganese(0) dimer $Mn_2(CO)_{10}$. The phosphorescence from the Pd(TPTBP) triplet state is quenched by $Mn_2(CO)_{10}$ via energy (or electron) transfer. In aerobic media, this photosensitization leads to complete labilization of the latter to release CO with a relatively small net Φ_{CO} (0.006). Since little CO release was seen in anaerobic media, the likely mechanism is cleavage of the $(CO)_5Mn\text{-}Mn(CO)_5$ bond followed by oxidative trapping of the resulting $Mn(CO)_5$ radicals and subsequent decomposition as shown for the dinuclear compounds described above. The manganese photoproduct was identified as MnO_2.

4. Two photon excitation:

The key disadvantage of each of the antenna-photoNORM conjugates shown in Figure 2 is that the strong absorption bands for the pendant chromophores all occur in the near-UV or visible wavelength regions that are non-ideal for treatment in deep tissue sites. In this context, we initiated a program to probe the possibility of utilizing *simultaneous* two-photon excitation (TPE) as a methodology to access excited states from which NO labilization may occur, as illustrated in Scheme 1. Although TPE had drawn attention in photodynamic therapy circles [72], Steve Wecksler in this laboratory was the first to utilize this technique with a photoNORM when he employed an ultrafast pulsed Ti/sapphire laser operating at 800 nm to demonstrate both upconverted emission and NO labilization from PPIX-RSE [24]. More quantitative studies with the red salt ester Fluor-RSE having two pendant fluorescein chromophores demonstrated a two-photon absorption cross section β of ~60 GM at 800 nm, about twice that for fluorescein itself [73]. Notably, the relationship between I_{abs} and I_i for simultaneous TPE is not linear as described above for single photon excitation. Instead I_{abs} is proportional to β c I_i^2 , where c is the concentration of the substrate of interest. Consistent with this relationship, Wecksler showed that a log-log plot of NO production versus the intensity of the laser pulse featured a slope of 1.8 ± 0.2 [73]. TPE production of NO with NIR has since been demonstrated with other Roussin's salt derivatives [74], with nitroaromatic derivatives [75], with a ruthenium nitrosyl complex [43] and with various nanomaterial constructs [76]

In addition to providing the opportunity to trigger NO release using tissue-penetrating near infrared light, TPE also has the potential for spatial resolution. Since the rate of a TPE stimulated photoprocess is a function of the square of the incident intensity, it will primarily occur at the focal point of the excitation beam. However, light scattering in passing through a heterogeneous structure may restrict the utility of this technique.

To our knowledge, there have been no reports of NIR two-photon stimulated CO delivery from a photoCORM, although this would appear to be a fairly simple experiment to test with some of the existing systems. There has been a recent report of using NIR TPE and detection for *in vivo* sensing of CO [77].

5. Quantum dot platforms.

We have also utilized semiconductor quantum dots (QDs) as antennas for photoNORM activation [26,78]. QDs offer enormous absorption cross sections for both single and two photon absorption as well as the ability to tune their spectra by varying the size of the semi-conductor core [79,80]. Furthermore, since QDs show strong photoluminescence (PL), one should be able to track their position in biological media. What is apparently the first example of QD photosensitization of NO release from a photoNORM, Dan Neuman and Alexis Ostrowski from this laboratory showed that CrONO quenches the PL from water soluble CdSe:ZnS and CdSeS:ZnS core:shell QDs concomitant with strongly enhanced NO release (Scheme 2) [26]. Peter Burks et al followed this study by probing the PL quenching and ultra-fast laser transient absorption kinetics for CdSeS:ZnS core:shell QDs in the presence of various chromium(III) complexes [81]. These properties were best interpreted in terms of Förster resonance energy transfer (FRET) from the QD band edge excited state to sensitize the spin-allowed quartet-to-quartet transition in these Cr(III) complexes. Subsequent intersystem crossing would give the Cr(III) doublet LF state discerned by time dependent density functional theory (DFT) calculations to be the reactive state (Figure 5) responsible for NO dissociation.

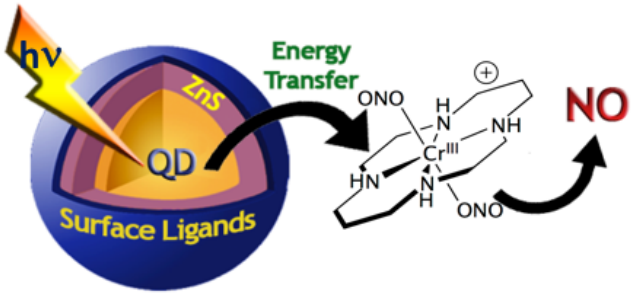

Scheme 2. QD to CrONO energy transfer. The surface ligands are dihydrolipoates to enhance water solubility [26].

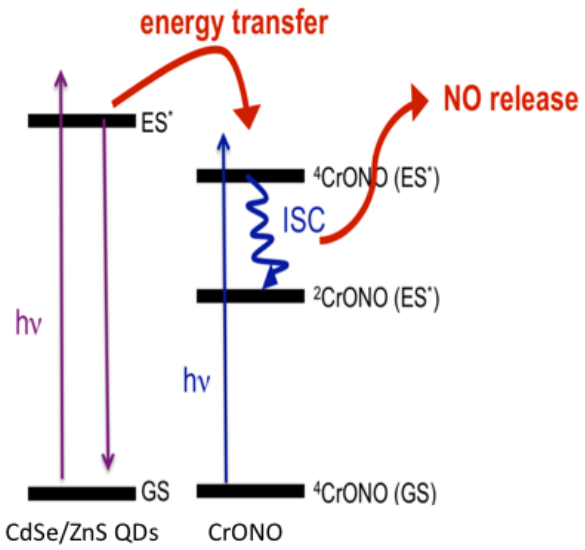

Figure 5. Energy level diagram for the photosensitization of *trans*-Cr(cyclam)$(ONO)_2^+$ by CdSe:ZnS core shell quantum dots in aqueous solution.

In collaboration with Roberto Santana da Silva, we demonstrated similar photo-sensitization of NO release by CdTe QDs (capped with mercaptopropionic acid to make them water soluble) and a ruthenium photoNORM *cis*-$[Ru\text{-}(NO)(4\text{-ampy})(bpy)_2]^{3+}$ (4-ampy = 4-aminopyridine) leading to markedly increased NO release with 530 nm excitation [78]. In this case, since there was little overlap of the QD emission and the Ru absorption bands, it was proposed that a charge transfer, rather than FRET mechanism was responsible. Transient spectra changes using ultrafast laser flash photolysis were consistent with this analysis. We have observed analogous photocatalytic charge transfer uncaging of carbon disulfide from the 1,1-dithiooxalate anion as photosensitized by CdSe QDs (eq. 6) [82].

$$S_2C{-}CO_2^{2-} \xrightarrow[\text{oxidant}]{\text{hv, QD}} CS_2 + CO_2 \qquad (6)$$

A problem with such QDs in terms of potential applications in human biology is the toxicity of cadmium. For this reason, we and others have turned attention to the synthesis of conjugates of photoNORMs to nanomaterials that are potentially less toxic. Wan and coworkers, for example have reported the synthesis of water dispersible nanoparticles (NPs) consisting of a Ag_2S QD cores conjugated to S-nitrosothiol derivatives such as the glutathiose derivative shown in Scheme 3 [83]. These nanomaterials were bifunctional since UV-visible irradiation (365 or 488 nm) of the conjugates in aqueous media resulted in NO release, while 808 nm excitation led to NIR PL that could be readily imaged with *in vitro* cells and *in vivo* in mice. The two processes were decoupled with the NO release attributed to the direct excitation of the RSNO functionality, which has been previously shown to be exceptionally photolabile to visible range excitation [84]. Virtually no nitric oxide release was seen upon NIR excitation.

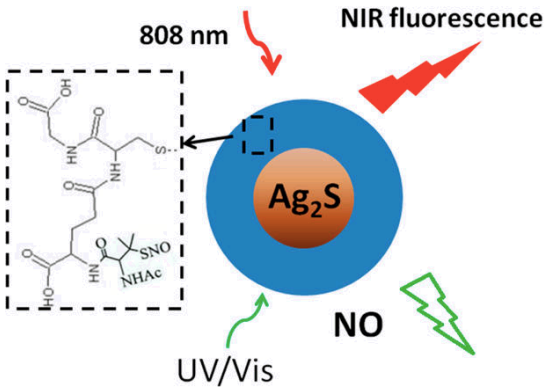

Scheme 3. Illustration of a nanomaterial consisting of a Ag_2S QD conjugated to a S-nitroso derivative of glutathiose showing how UV/Vis excitation leads to NO release while 808 nm excitation leads to imageable NIR fluorescence. (Reprinted with permission from ref. 83a, Copyright 2013, American Chemical Society)

A seemingly ideal QD semiconductor material for biological applications would be carbon; thus, there has been a growing interest in graphitic nanomaterial photosensitizers [85-87]. For example, Scheme 4 illustrates a conjugate of carbon quantum dots (CQDs) linked covalently to a nitroaniline-based NO photodonor prepared by Sortino and coworkers [85]. Single photon excitation was limited by the absorption of this conjugate at wavelengths less than 450 nm. However, the high two photon cross section of these CQDs allowed NO photo–uncaging via FRET activation of the nitroaniline derivative after TPE with 800 nm light. This combination proved toxic to HeLa cells *in vitro* and after intra-tumoral injection modestly reduced the size of hypoxic human pancreatic BxPC-3 tumors induced in Balb/c SCID mice.

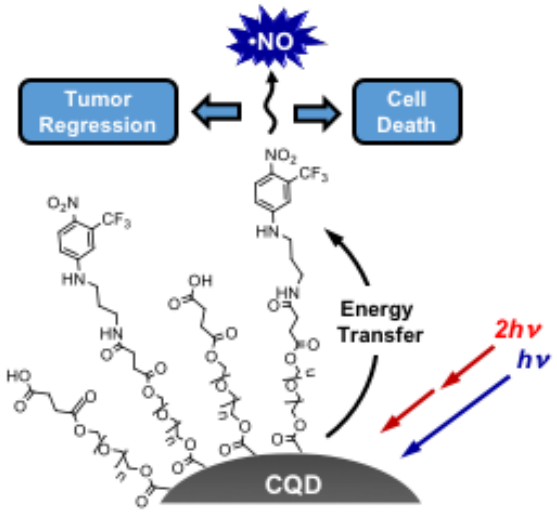

Scheme 4. Illustration of a carbon quantum dot decorated with nitroaniline derivatives that are photoactivated by FRET from the CQD excited state formed by single or two photon excitation. (Adapted with permission from ref. 85)

Lui et al [86] have described several luminescent nanoplatforms consisting of N-doped graphene QDs (GQDs, diameters 7-10 nm) functionalized with a ruthenium photoNORM (77,78). For example, the nanoplatform illustrated in Scheme 5 is also decorated with a

triphenylphosphonium moiety that, when administered to HeLa cancer cells, directs this platform to localize in the mitochondria [86]. The *in vitro* generation of nitric oxide in these cells upon 808 nm irradiation was demonstrated using the intracellular NO-sensitive fluorescent probe, DAF-FM DA (4-amino-5-methylamino-2',7'-difluorofluorescein diacetate). Furthermore, this treatment significantly decreased the viability of these HeLa cells by triggering apoptosis. Similar effects were noted after intratumoral injection of this platform into HeLa tumor-bearing mice followed by 808 nm irradiation. Notably, continuous 808 nm irradiation of a 1 mg mL^{-1} suspension of this nanoplatform in aqueous buffer at a 1 watt per cm^{-2} power density for 10 min led to a substantial temperature change in the bulk solvent. Such a photothermal effect needs to be considered whenever such absorbers are subjected to continuous NIR excitation. The total energy deposited at a site is likely to be much larger under such conditions than when using a pulsed laser with much higher peak power, but lower average power.

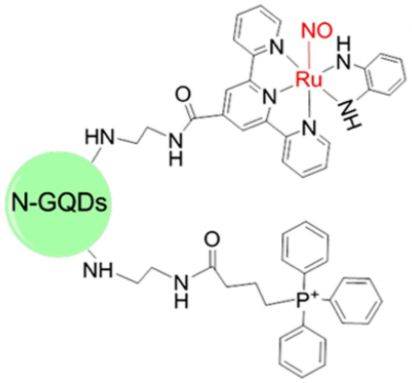

Scheme 5. Cartoon illustrating the covalent attachment of both a ruthenium photoNORM and a triphenylphosphonium moiety on a N-doped graphene QD. (Adapted with permission from reference 86).

The same research team has also recently reported another platform based on N-doped graphene QDs decorated with a ruthenium photoNORM and a galactose derivative that selectively targets liver cancer cells over normal liver cells (87).

Po-Ju Huang of this laboratory has also developed a nano-carrier with N-doped graphene QDs as the photo-active cores with 4 nm diameters and 1.4 nm thick [88]. Through amide coupling of surface carboxylates with oleylamine, the resulting GQDs had lipophilic surface domains that could be assembled with the amphiphilic biotinylated phospholipid-functionalized poly(ethylene glycol) DSPE-PEG to give the nanocarrier GQD@ DSPE-PEG. This construct was surface modified with HIV-1-Trans-Activator of Transcription (TAT) peptide, a well-known [89] cell-penetrating peptide, via biotin-streptavidin-biotin assembly strategy. Nano-carriers surface modified in this manner can overcome cellular membrane barriers to enter cells (Scheme 6). The lipophilic domains of the these nano-carriers were loaded with a hydrophobic CrONO derivative *trans*-$[Cr(PetA)(ONO)_2]BPh_4$ (PetACrONO, PetA = 5,12-dimethyl-7,14-diphenyl-1,4,8,11-tetraaza-cyclotetradecane). The fully loaded nanocarriers largely fell in the 20-70 nm size range.

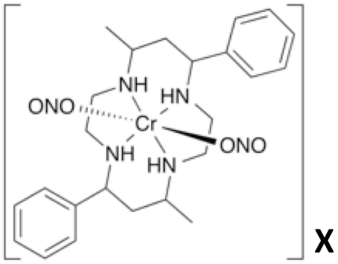

PetACrONO

An aqueous suspension of these GQD@DSPE-PEG nano-carriers loaded with PetACrONO in pH 7.4 PBS solution release NO upon continuous excitation at 794 nm with a diode laser. Notably, in solution this Cr(III) complex displays no absorbance at 794 nm nor is it photoactive at this wavelength. The released NO was quantified as functions of irradiation time and of laser power density using a Sievers nitric oxide analyzer (NOA). The quantity of NO generated was approximately linear in both laser power and irradiation time [88]. These observations argue against NO release from the incorporated PetACrONO occurring through multi-photon processes sensitized by the GQD cores. Thus, it seems likely that a photothermal process is triggering the NO release from the photoNORMs located in the lipophilic domains.

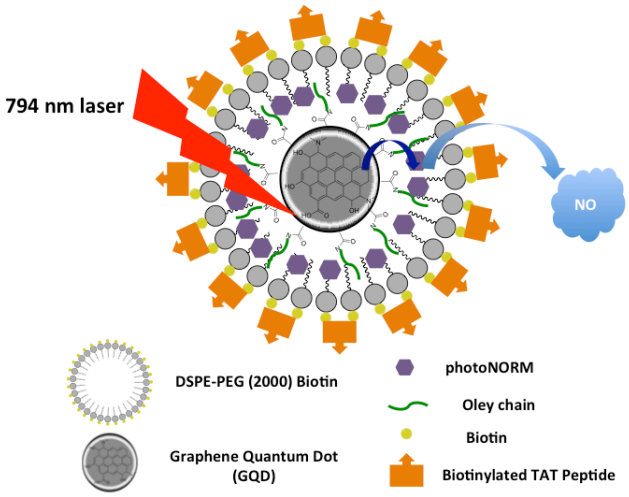

Scheme 6. Illustration of the loading of PetACrONO into the lipophilic domains of the nanocarrier GQDs@DSPE-PEG, the surface of which can be conjugated with biotinlyated TAT peptide to enhance the internalization into cancer cells (Reproduced with permission from ref. 88)

A preliminary *in vitro* study showed that TAT modified GQD@DSPE-PEG nanocarriers containing PetACrONO can be delivered into HeLa cells [88]. The HeLa cells had been pretreated with the nitric oxide synthase inhibitor, L-N-nitroarginine methyl ester to minimize native NO generation. After 2 min irradiation of cells loaded with these NO-nanocarriers at 794 nm with power density of 13 W/cm^2, a strong fluorescent signal from the intracellular NO-probe DAF-FM DA was evident. In contrast, there was negligible fluorescence from control experiments including those cells with the PetACrONO containing nanocarriers that were not subjected to NIR excitation.

Ruggi and Zobi [90] have described the synthesis and photochemistry of several conjugates between CdSe:ZnS core shell QDs and Mn(I) photoCORMs of the type fac-$Mn(CO)_3$(LL)Br, where LL is a bipyridine derivative. Carboxylate or dithiocarbamate functionalities on the LL ligand facilitated attachment to the surface of QDs with a band edge absorption at 504 nm. Visible excitation of these QD-photoCORM conjugates at 510 nm, led to CO photodissociation at rates 2 to 6-fold faster than the analogous photoreactions of these fac-$Mn(CO)_3$(LL)Br photoCORMs alone, presumably because of the much higher absorbance at this wavelength for the former. This study was the first and, apparently, the only report to date of photoCORM sensitization by a semiconductor QD [91].

6. Polymer, metallic and other nanomaterial platforms:

Another nano-material strategy for the delivery of photoNORMs is to utilize organic polymers materials as nanocarriers for the caged SMB precursors. Tfouni et al demonstrated this by encapsulating the ruthenium nitrosyl photoNORMs trans-Ru(NO)Cl(cyclam)]$(PF_6)_2$ and [Ru(NO)(Hedta)] (Hedta = ethylenediaminetetraacetic acid) in poly(D,L-lactic-co-glycolic) acid (PLGA) nanoparticles (220-820 nm diameter) [34d]. The loaded PLGA NPs showed lower *in vitro* toxicity against melanoma cells relative to the same ruthenium nitrosyls in solution. UV irradiation (300-350 nm) led to NO release and considerable surface damage to these cells with rupture of the plasma membranes indicating that NO generated in the PLGA NPs can readily escape.

Sortino and coworkers have very creatively engineered polymer nanomaterials containing various nitoaromatics as photoNORMs as well as combinations of various fluorophores [37b, 37c, 37e, 37f]. In this manner, these researchers were able to combine several functions including NO release, photodynamic production of singlet oxygen, and theranostic reporting of the location and timing of NO release. These studies have been recently the subject of an extensive review by Fraix, Marino and Sortino [37d].

Liposomes, although somewhat larger than typical nanoparticles, have also been examined as possible vehicles for delivering photoNORMs to specific targets. For example, Ostrowski et al [63] encapsulated the BF_4^- salts of CrONO and the anthracene tethered complex Anth-CrONO (Figures 1 & 2) in phosphatidylcholine liposomes (Scheme 7). The fluorescence of Anth-CrONO can be detected through the liposomes, thus these vessels can be tracked simultaneously with therapeutic NO release. The quantum yield for net NO release from these liposome-encapsulated complexes in oxygenated solution proved to be considerably larger for than for the same species free in solution, presumably owing to changes in the dynamics of post photolysis reactions that scavenge this photoproduct. Since the enhanced permeation and retention (EPR) effect accumulates nano-sized particles such as liposomes in tumors (92), liposomes loaded with a luminescent photoNORM have theranostic potential.

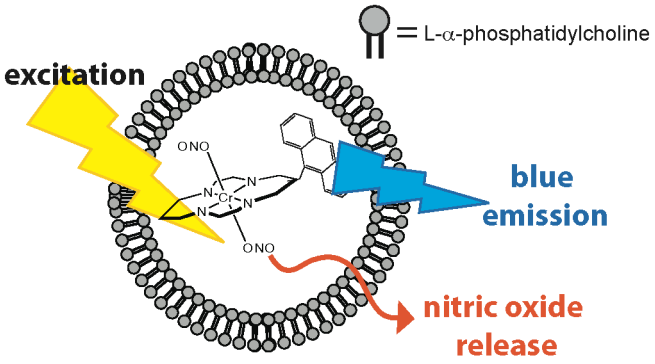

Scheme 7. Illustration of a liposome encapsulating the luminescent salt [Anth-CrONO]BF_4 . Photolysis leads both to NO release and detectable emission. (Reprinted with permission from ref 63. Copyright 2012 American Chemical Society).

Nakanishi et al (93) have described another example of a photoNORM loaded liposome. In this case, the lipophilic Ru salen complex [Ru(L)Cl(NO)] with pendant cholesterol groups (L = N,N'-ethylene-bis(4-cholesteryl-hemisuccinate-salicylideneamine) was incorporated into bilayers of a 1,2-ditetradecanoyl-sn-glycero-3-phospho-(1'-rac-glycerol) liposome. Irradiation at 495 nm led to NO release detected using the NO probe DAF-2 in coexisting liposomes.

Several features of metallic nanoparticles are attractive as platforms for drug delivery. One is the affinity of metals such as gold for thiols that facilitates the simultaneous assembly of different theranostic functionalities, such as bioimaging and targeted drug delivery in a single NP [94]. So far, applications of this technology to NO uncaging are relatively limited, but the plasmonic absorptions of gold NPs in the NIR and the resulting photothermal effects offer some very interesting possibilities in this regard.

Sortino and coworkers were the first to explore NO release from systems constructed from metallic nanoparticles when they used platinum NPs as the core to assemble a polyfunctional system containing both a porphyrin based fluorophore and a derivative of nitroaniline as a photoNORM [95,96]. Irradiation of this ensemble in pH 7.4 aqueous solution at 400 nm gave both NO release and red fluorescence. They have extended this approach by using gold NPs as the core for sophisticated water-soluble ensembles for photo-activated NO release [96]. In each case, the photoNORM was a derivative of nitroaniline and the activating light was in the visible range (> 400 nm).

In collaboration with colleague Norbert Reich, Liz Levy of this laboratory utilized the NIR plasmonic absorption properties of hollow gold nanoshells (HGNs, ~65 nm diameters) to photo-uncage NO from an ensemble built on a HGN core [32]. The nitric oxide precursor in this case was TCF, a thiol functionalized derivative of cupferron, (ammonium **N**-nitroso(4-mercapto-methylphenyl)hydroxylamine) coordinated to the HGN surface. Aqueous solubility was achieved by adding thiolated polyethylene glycol (TPEG) ligands [97] The resulting TCF-HGN-TPEG conjugate displayed a broad, very strong absorption band centered at ~750 nm attributed to the plasmonic transition of the HGN core. Nitric oxide release was triggered by 800 nm excitation of this conjugate (Scheme 8) using the pulses from an ultra-fast laser. The high peak intensities of the laser pulses are exceptionally effective in the rapid heating of gold NPs with NIR light [94a],

so we attribute this reactivity to the photothermal decomposition of the TCF. Remarkably, aqueous solutions of these TCF-HGN-TPEG conjugates could also be activated by a continuous diode laser operating at 800 nm, although it was necessary to focus the beam to a diameter of 0.9 mm in order to generate sufficient intensity for this nonlinear process.

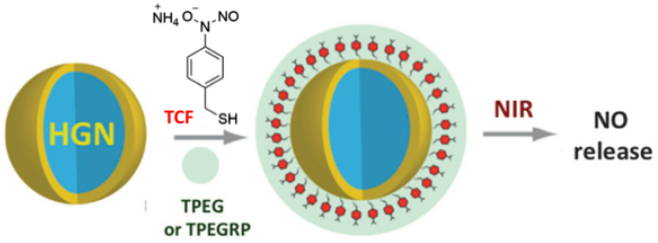

Scheme 8. HGN surfaces are coated by co-absorption of TCF and TPEG or TPEGRP. The TPEGRP includes a cell-targeting peptide. Laser excitation (800 nm) of these conjugates results in NO release with spatial-temporal control.

The HGN platform also allowed for functionalizing the gold surface with a thiolated polyethylene glycol modified to include the terminally bound targeting peptide RPARPAR (TPEGRP). The RPARPAR peptide mediates cellular internalization via endocytosis only for cells that overexpress the Neuropilin-1 receptor [98]. Thus, the TCF–HGN–TPEGRP conjugates were readily internalized by PPC-1 or 22Rv1 prostate carcinoma cells, but not by HeLa cells that lack this receptor. Photoexcitation of 22Rv1 containing the internalized TCF–HGN–TPEGRP conjugates demonstrated NO release as reported by the intracellular NO-probe DAF-FM DA [32].

Although not strictly a photothermal effect, Janiak and coworkers [99] prepared conjugates consisting of Fe_2O_3 nanoparticles to which they have attached the ruthenium carbonyl complex $Ru(CO)_3(L)Cl$, where L is a phenylalaninato derivative. These are coated with dextrin to enhance water solubility. At physiological temperatures $Ru(CO)_3(L)Cl$ conjugate releases CO slowly (that is, it is a CORM), however the rate of CO release is markedly accelerated when the iron oxide nanoparticles of these ensembles are heated by an alternating current magnetic field.

A somewhat different approach was taken by Furukawa and coworkers [100], who immobilized the manganese photoCORM *fac*-MnBr(bpydc)$(CO)_3$ (bpydc = 5,5'-dicarboxylate-2,2'-bipyridine) into a nanocrystalline Zr(IV)-based metal–organic framework (MOF). The resulting MOF crystals were photoactive toward carbon monoxide release when irradiated with 460 nm light. These MOF crystals were suspended in a biocompatible polymer matrix (PDMS) upon which were grown HeLa cells. Visible photolysis of this matrix led to CO release and up take into the cells as demonstrated using the intracellular fluorescent CO-probe COP-1 [101]. The photosensitive polymer incorporated MOFs with high CO payloads would appear to be appropriate for localized applications as implants or other devices.

Schoenfisch and coworkers [102], among others [103], have used silica nanoparticles as a delivery method for NO-releasing compounds. Several recent studies (29, 104, 105) have demonstrated the use of similar silica-based NPs for photoNORM and photoCORM delivery agents. As will be discussed in the next section, Garcia et al (29) prepared mesoporous silica NPs with a NIR-photoactive core consisting of a upconverting NP (UCNP Figure 6. This was loaded with the photoNORM Roussin's black salt ($Na[Fe_4S_3(NO)_7]$ then coated with an amphiphilic

polymer to seal the pores. The result was a water-soluble nanocarrier that released NO upon excitation at 980 nm.

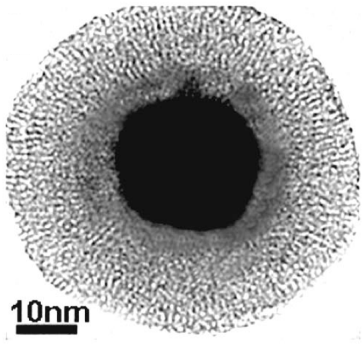

Figure 6. TEM image of a mesoporous silica nanoparticle with an upconverting NP core (adapted from ref. 29)

A different approach was taken by the Sortino group (104) who embedded luminescent carbon quantum dots into amine terminated mesoporous silica NPs. This material was then functionalized by reacting with 4-chloro-2-trifluoromethyl-nitrobenzene to give a covalently linked nitroaniline derivative on the surface of these ~400 nm diameter constructs. Photoexcitation of an aqueous suspension of these conjugates with 405 nm light led to a bleaching of characteristic absorption band of the nitroaniline derivative and release of NO. On the same time scale, the CQD emission, which was largely quenched in the nitroaniline derivative, was restored thereby acting as an optical reporter of NO release.

In a similar fashion, Chakraborty et al (105) prepared mesoporous silica nanoparticles (100 nm diameter) packed with a designed photoCORM *fac*-[$Re(CO)_3(pbt)(PPh_3)$](CF_3SO_3) that is strongly luminescent at 605 nm when excited in the UV. In vitro experiments showed that these constructs were endocytosed into human breast cancer cells (MDA-MB-231) where they were visualized by their luminescence. Exposure of the cells to UV excitation led to reduced emission owing to CO release from the Re(I) compound and to death of the MDA-MB-231 cells attributed to CO-induced toxicity.

7. Upconverting nanoparticles (UCNPs*)* antennas*.*

Lanthanide-doped UCNPs represent an exciting change in the landscape of biological imaging and photosensitization owing to their unique optical properties and *low toxicities* [106]. These can effect NIR-to-visible (or UV) up-conversion by *sequential* multi-photon excitation which is inherently more efficient than simultaneous two photon excitation [107]. In the core UCNPs, one lanthanide ion (Ln^{3+}), typically Yb^{3+}, acts as the light absorbing sensitizer while a second, such as Er^{3+} or Tm^{3+}, is the emitter after sequential energy transfer from the sensitizer. Thus, upconversion requires much lower light intensities than does simultaneous TPE, so one can use relatively simple NIR diode lasers operating in pulsed or continuous wave (CW) modes to effect such excitation. The upconversion efficiency remains a function of I^n with $n > 1$, so the excitation efficiency is greatest at the focal point and spatial resolution remains a potential feature. Thus, the ability to effect uncaging with NIR light from a simple CW diode laser is a potential game changer in photo-activated drug delivery [108].

Recognizing that UCNPs would be attractive as NIR photosensitizers with photoNORMs, John Garcia of this laboratory, in collaboration with colleague Galen Stucky and Fan Zhang and Dongyuan Zhao of Fudan U used, for the first time, UCNPs to photosensitize NO uncaging with NIR light [29]. These UCNPs, composed of $NaYF_4$:Yb/Er cores (~10 nm) coated with $NaYF_4$ and mesoporous silica shells displayed bright visible luminescence upon 980 nm irradiation with a CW diode laser. The mesoporous silica shell was infused with the photoNORM Roussin's black salt (RBS), then capped with poly(allylamine hydrochloride) to inhibit RBS diffusion into the solution. This procedure gave a nano-carrier that released biologically relevant concentrations of NO when photolyzed at 980 nm in aqueous solution owing to the overlap of the upconverted emission and the RBS absorption spectrum (Figure 7). Notably, RBS undergoes NO photodissociation when irradiated directly with visible light (eq. 7) [20] but is not when irradiated directly at NIR wavelengths [29].

$$Fe_4S_3(NO)_7^- \xrightarrow[O_2]{h\nu} 3.9\ Fe^{2+} + 5.9\ NO + 3\ S^{2-} + \text{other products} \qquad (7)$$

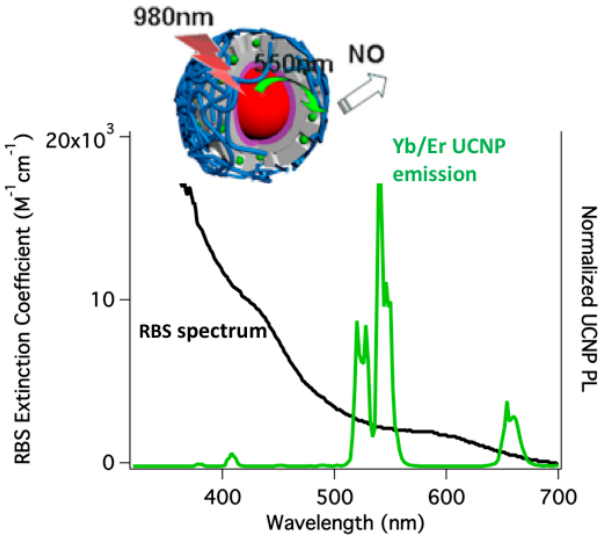

Figure 7. The overlap of the upconversion emission spectrum water soluble $NaYF_4$:Yb/Er@SiO_2@mpSiO_2 UCNP with the absorption spectrum of RBS. *Insert*: Illustration of a nanocarrier with a UCNP core and a mesoporous silica shell loaded with the photoNORM RBS and capped with an amphiphilic polymer. NIR photolysis results in NO uncaging.

Although the mechanism has not been studied in detail, energy transfer likely occurs by visible light emission from the UCNP followed by reabsorption by the photoNORM (the so-called "trivial" mechanism). While inefficient, this pathway simply requires that the precursor have strong absorption bands that overlap with the UCNP emissions as shown in Figure 7. This simple requirement led Peter Burks and John Garcia of this laboratory to prepare mm-sized polymer disks from biocompatible polydimethylsiloxane (PDMS) in which UCNP is simply suspended in the curing polymer and the photoNORM RBS was infused into the cured disk (Figure 8). NO release as measured with the NOA was effected by 980 nm irradiation with the CW diode laser, although

in order to obtain reproducible data, they developed a device that scans the entire disk with an oscillating beam (Figure 9) [30]. Furthermore, they demonstrated that NIR excitation triggered photo-uncaging from these devices even through tissue filters [30]. One can envision using such materials as implants.

Figure 8. PDMS disks (5 x 2 mm). *Left:* blank disk. *Right*: disk loaded with UNCPs and RBS. Pictured with a US 1 cent coin to indicate relative size.

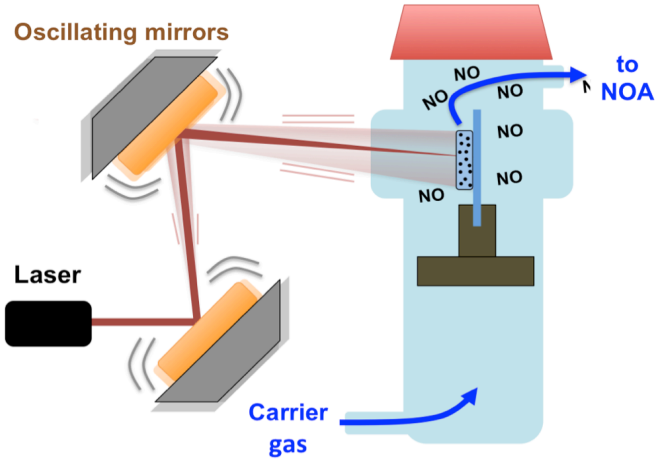

Figure 9. Apparatus for evaluating NO release from photoNORMs in polymer disks. The oscillating mirrors are controlled in such a manner that the laser beam systematically samples the entire sample.

We have extended these studies by demonstrating NO release from disks prepared with different commercial formulations of biocompatible silicon polymers in which were suspended Nd^{3+} sensitized UCNPs (β-$NaYF_4$:Tm/Nd/Yb/Gd@$NaYF_4$:Nd) that can be activated at 800 nm. The photoNORM infused into the disk was the hydrophobic complex PetACrONO [109]. Independent studies by Ostrowski et al [110] with related silicone polymer disks containing UCNPs and the hydrophobic CrONO salt *trans*-[Cr(cyclam)$(ONO)_2$]BPh_4 gave similar results. The latter researchers also made the important discovery that the facility of NO escape from the polymer was quite sensitive to the manner in which the photoNORM was incorporated into the disk.

Multiphoton excitation of UCNPs also offers a method for the NIR photoexcitation of photoCORMs. For example, the Mn(I) photoCORM *trans*-$Mn(CO)_2(PPh_3)_2(bpy)^+$ displays strong visible range absorptions, 470 nm photolysis of which leads to facile release of both CO's with a moderately high quantum yield (0.26). The spectrum is well suited for matching the emission from $NaYF_4(Yb_{20}Tm_{0.2})$ UCNPs (Figure 10). To take advantage, Agustin Pierri from this laboratory

in collaboration with Nanfeng Zheng of Xiamen University [46] assembled nano-carriers consisting of UCNP cores terminated with hydrophobic oleate surface ligands made water-soluble by coating with an amphiphilic phospholipid-functionalized poly-(ethylene glycol) (DSPE-PEG 2000) (Figure 11). The resulting nano-carrier provided a lipid-like interior into which the hydrophobic salt *trans*-$[Mn(CO)_2(PPh_3)_2(bpy)](CF_3SO_3)$ was readily infused to bring together the UCNP NIR antenna and a hydrophobic photoCORM in a stable, water-soluble ensemble. Dynamic light scattering measurements showed these to have diameters largely in the 16–30 nm range. NIR excitation (980 nm) of an aqueous solution containing the resulting loaded nano-carrier led to CO release as confirmed by gas chromatography [44] and by trapping with deoxymyoglobin [67].

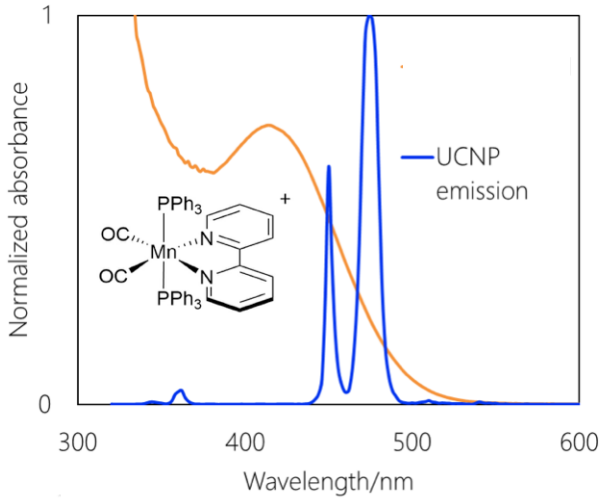

Figure 10. Absorption spectrum for *trans*-$Mn(CO)_2(PPh_3)_2(bpy)^+$ and emission spectrum of $NaGdF_4$:Tm,Yb@$NaGdF_4$ UCNPs (λ_{irr} = 980 nm).

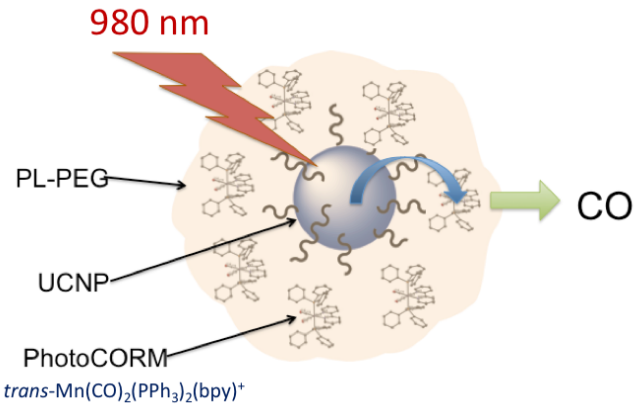

Figure 11. Water-soluble photoCORM nano-carriers with a UCNP core

A similar approach to activating a photoCORM by NIR-to-visible upconversion has recently been reported by X. Liu and coworkers [111]. These researchers constructed a nanocarrier with a $NaYF_4$:Yb/Er UCNP core coated with silica and surface functionalized with thiol groups on the by treating the $NaYF_4$:Yb/Er-SiO_2 UCNPs with 3-mercaptopropyltrimethoxysilane. Reaction of the surface SH groups with $Fe(\eta^5\text{-}C_5H_5)(CO)_2I$ led to the fixation of "$Fe(\eta^5\text{-}C_5H_5)(CO)_2$" presumably by

thiol displacement of the coordinated iodide as evidenced by the IR spectra of the resulting conjugates. NIR photolysis of the $NaYF_4$:Yb/Er-SiO_2-CORM conjugates with 980 nm light led to visible emission bands like those seen in Figure 6 that overlap with the absorption spectrum of the iron carbonyl unit. Photo-induced CO release was evidenced by changes in the IR spectrum, but it does not appear that the freed CO was directly measured. The $NaYF_4$:Yb/Er-SiO_2-CORM conjugate was not toxic to human umbilical vein epithelial cells (HUVEC) or mouse fibroblast cells (L929) nor did it prove phototoxic when irradiated at 980 nm.

8. Biological targeting

While NIR excitation allows one to define location and timing of SMB uncaging in tissue, another key task is to improve transport of the precursor-antenna conjugates to the desired targets. Such targeting can be accomplished by direct injection into the desired site or by implanting a device such as a PDMS disk such as shown in Figure 7 or some other solid material incorporating the caged SMB. Indeed, if such an implant were attached to an optical fiber [51b, 112], there would be less of a restriction to making the specific photoNORM or photoCORM responsive to tissue-transmitting wavelengths. More elegant strategies would be to recruit the specificity of biological mechanisms to target the tissues of interest. Recent examples include building conjugates with a triphenylphosphonium [86] or folic acid groups to address receptors overexpressed by certain cells [113].

In this laboratory, we approached this challenge in two ways. The first was introduced above, namely to use targeting peptides to direct water-soluble nanoparticle carriers to cell types with specific receptors [32]. In that example, a conjugate was assembled on the hollow gold nanoparticle platform that included the terminally bound targeting peptide RPARPAR that mediates cellular internalization only for cells that overexpress the Neuropilin-1 receptor [99]. *In vitro* microscopy experiments showed these conjugates to be readily internalized by PPC-1 or 22Rv1 prostate cancer cells, but not by HeLa cells lacking this receptor. NIR photolysis of nanocarriers internalized in 22Rv1 clearly demonstrated intracellular NO-release [32]. Depending on the sequences, such RGD peptides target specific cell types, both *in vitro* and *in vivo* [99,114]. Tirrell et al, for example, used micelles constructed of peptide terminated polymers for targeted delivery of chemotherapeutic agents to malignant giomas, thereby minimizing other side effects [115]. Simply stated, these proof-of-principle precedents suggest that decorating other photoNORM or photoCORM nanocarriers with the appropriate targeting peptide may greatly enhance delivery specificity.

The second approach is to recruit immune cells to serve as Trojan horses to carry the desired payload to the targeted tissue (Scheme 9) [33]. In collaboration with BioEngineering colleague

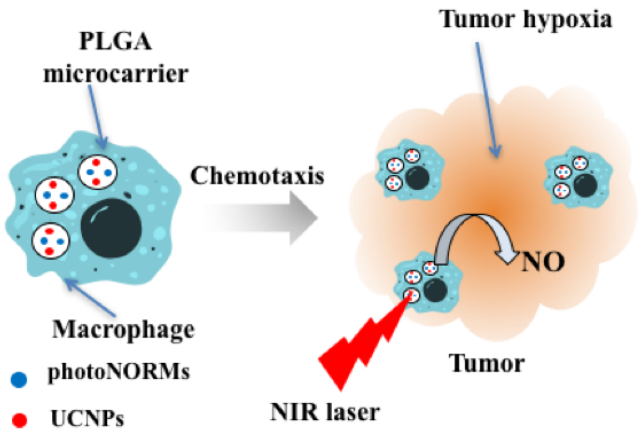

Scheme 9. Trojan horse mechanism using macrophages to transport PLGA microcarriers loaded with UCNPs and a photoNORM to tumors or other sites of inflammation.

Samir Mitragotri, Michael Evans and Po-Ju Huang in this laboratory initiated a program to probe the ability of macrophages and monocytes to carry loaded micron-sized polymer carriers to target sites [33]. Our micro-carriers are miniaturized versions of the biocompatible polymer disks described above [30]. Earlier work showed that these immune cells will ingest micron-sized particles and transport them to sites of inflammation [116,117]. Unlike other circulatory cells, monocytes can cross typically impenetrable barriers such as the blood brain barrier [118] and can accumulate in difficult-to-access tissues, such as tumors [119,120]. Tumor hypoxia generates inflammatory signals that recruit monocytes and macrophages from the blood *via* chemotaxis.. Thus, our premise was that these micro-carriers can be loaded with a photoNORM and UCNP antennas and that immune cells can be recruited to serve as Trojan horses to transport them. Once the precursors are deposited in the targeted tissue, the relevant SMB is uncaged by NIR excitation.

To address this proposal, we prepared micro-carriers from the bio-degradable polymer PLGA and loaded these with UCNPs and hydrophobic photoNORMs such as PetACrONO and the [Mn(NO)dpaq^{NO2}]BPh$_4$ provided by Yutaka Hitomi [54b]. NIR irradiation of aqueous suspensions of these microparticles released NO as measured using an NOA and demonstrated that NO can escape the particles. Furthermore, *c*onfocal microscopy showed that murine macrophages ingest these micron sized PLGA beads and that ingestion efficiency improved significantly when IgG antibodies were incorporated in the preparation of these particles. Photolysis of macrophages containing ingested, loaded micro-carriers leads to intracellular NO release as imaged using the DAF-FM-2DA fluorescent reporter.

The loaded microparticles proved to be non-toxic to their bone marrow derived macrophage hosts in the absence of light. These cells also maintained their chemotactic ability to traverse an *in vitro* brain barrier transendothelial model. Furthermore, this study showed that the microparticle-carrying macrophages deeply penetrate into NIH-3T3/4T1 spheroid tumor models that were grown for this purpose [33]. Both the [Mn(NO)dpaq^{NO2}]BPh$_4$ photoNORM and the Nd-UCNPs are activated by NIR excitation at ~800 nm; thus, simultaneous therapeutic NO delivery and photoluminescence (PL) imaging can be achieved with a NIR diode laser. Irradiation of the infiltrated tumor spheroids with 794 nm light led to quantifiable NO release and emission from

the Nd-UCNPs that gave images of microparticle location. When the NIR light doses were relatively low, there was a reduction in hypoxia inducible factor 1 alpha (HIF-1α) levels in the tumor spheroids. In contrast, high doses led to cell death, presumably by triggering an apoptosis mechanism. Thus, we were able to recruit macrophages as Trojan Horses to carry PLGA-based microparticles with a NIR-activated theranostic payload into a tumor model and were able to control biological response by varying the amount of irradiation, thus the dosage of SMB. This strategy addresses challenges often faced with therapeutic administration of NO and offers multiple treatment pathways applicable to the uncaging of other small molecule bioregulators and/or therapeutic drugs.

9. Summary

Research into the uncaging of NO and CO has progressed from designing new photoNORMs and photoCORMs that can deliver these payloads with controllable photochemical rates to developing strategies to release these SMBs at specific physiological targets. The general lessons learned define parameters that allow one to use longer wavelength excitation to activate photo-uncaging and to recruit biological mechanisms to facilitate such specificity. Such lessons are readily translated to the delivery of other biologically active small molecules. It remains to be seen when these accomplishments will transition into *in vivo* studies and eventually to the clinic.

10. Abbreviations:

bpy	2,2'-bipyridine
CORM	Carbon monoxide releasing moiety
CrONO	*trans*-Cr^{III}(cyclam)$(ONO)_2^+$
CW	Continuous wave
cyclam	1,4,8,11 tetraazacyclotetradecane
DAF-FM DA	4-amino-5-methylamino-2',7'-difluorofluorescein diacetate
DFT	Density functional theory
DMSO	Dimethylsulfoxide
$dpaq^{NO2}$	2-[*N*,*N*-bis(pyridin-2-ylmethyl)]-amino-*N*'-5-nitro-quinolin-8-yl-acetamido)
DSPE-PEG	Phospholipid-functionalized poly(ethylene glycol)
ES	Excited state
Fluor	Fluorescein
FRET	Förster resonance energy transfer
gly^-	Glycinato
GM	Goeppert-Mayer unit for two photon absorption
GSH	Glutathione
HGN	Hollow gold nanosphere
HO	Heme oxygenase
I_i	Incident light intensity
I_{abs}	Intensity of light absorbed
IR	Infrared

LF	Ligand field
Mb	Myoglobin
MLCT	Metal to ligand charge transfer
NIR	Near infrared
NMR	Nuclear magnetic resonance
NOA	Sievers mitric oxide analyzer
NP	Nanoparticle
PDMS	Polydimethylsiloxane
PEG	Polyethylene glycol
PetA	5,12-Dimethyl-7,14-diphenyl-1,4,8,11-tetra-aza-cyclotetradecane.
phen	1,10-Phenanthroline
photoCORM	Photo-activated CO releasing moiety
photoNORM	Photo-activated NO releasing moiety
PL	Photoluminescence
PLGA	Poly(D,L-lactic-co-glycolic) acid
Por	Porphyrin
PPIX	Protoporphyrin-IX
py	Pyridine
QD	Quantum dot
R_i	photochemical rate
RBS	Roussin's black salts
RRS	Roussin's red salt
RSE	Roussin's red ester
salen	N,N'-ethylenebis(salicylideneiminato)dianion
Salophen	N,N'-1,2-phenylenebis(salicylideneiminato)dianion
TCF	Thiol functionalized derivative of cupferron
TD-DFT	Time-dependent density functional theory
TMOS	Tetramethylorthosilicate
TPE	Two-photon excitation
TPPTS	Tris(sulfonatophenyl)phosphine trianion
UCNP	Upconverting nanoparticle
UV	Ultraviolet
Φ	quantum yield
λ_{irr}	irradiation wavelength
β	two-photon absorption cross section

11. Acknowledgements:

Research at UC Santa Barbara into the biologically relevant chemistry and photochemical delivery of SMBs has long been supported by the Chemistry Division of the US National Science Foundation, most recently through grant number NSF-CHE-156570. I want to especially acknowledge the two most recent Ph.D. graduates from the research group, Drs. Po-Ju Huang and Zhi Li,

12. Appendix: Discussion of "first order rate laws" in photochemical reactions.

Excited states may deactivate by multiple unimolecular pathways including internal conversion / intersystem crossing to other excited states, nonradiative or radiative decay to the ground state and reaction to products. In addition, one must consider quenching by other species including bimolecular energy or electron transfer in solutions or unimolecular energy or electron transfer in polychromophoric systems [121]. Elucidating the trajectories, dynamics and mechanisms of such pathways, which in many cases are exceedingly fast, requires sophisticated application of flash and continuous photolysis techniques, and such issues continue to be of active interest to photochemists and photophysicists.

This investigator believes that understanding the fundamental mechanisms of excited state chemistry is quite relevant to designing better precursors for the photo-uncaging of bioactive substances such as the small molecule bioregulators (SMBs) discussed in this article. However, it is clear that what drives the activity in this field is the design of new molecules, materials or strategies for the delivery of such agents to the targets of interest. The key question in such an application is -- Does it work for the intended purpose? In this context, once the caged SMB (or other bioactive compound) is localized at the desired site, the rate and dosage of delivery is of crucial importance. For a material that releases the SMB by a unimolecular photochemical process, that rate is the product of the quantum yield of SMB uncaging Φ_{SMB} times the intensity of the light absorbed (I_{abs}) by the SMB precursor (eq. A1)

$$\text{SMB uncaging rate} = d[SMB]/dt = \Phi_{SMB} \, x \, I_{abs} \qquad \text{(A1)}$$

where I_{abs} is generally defined for solution phase studies in terms of the Einsteins (moles) or number of quanta absorbed by the photoreactant per unit volume per unit time [122].

The quantum yield Φ_i is a unit-less efficiency term that can be defined for a specific photoprocess *i* :

$$\Phi_i = \text{(number of molecules undergoing process i)/(number of photons absorbed)} \qquad \text{(A2)}$$

This term indicates how excited states initially formed by the light absorption partition between the various deactivation and reaction pathways under the specific conditions. For a solution, where the photoreactant is the only species absorbing the incident light, I_{abs} is defined by eq. A3.

$$I_{abs} = I_i \, (1\text{-}10^{-Abs(\lambda_i)}) \qquad \text{(A3)}$$

where I_i is the incident light intensity. Abs(λ) is the solution absorbance of the substrate X at irradiation wavelength λ_{irr} and equals the product of the molar concentration of X, the molar extinction coefficient (ε_λ, in L moles^{-1} cm^{-1}) at λ_{irr} and the pathlength *l* of the cell (in cm).

An unfortunate development has been the tendency of some workers in the field to report a first order rate constant (k_p) for the photochemical SMB uncaging from a specific precursor X (i.e., photochemical rate = k_p[X]). Such "rate constants" were obtained from exponential plots of optical absorbance changes during the course of uncaging. The problem with such plots is that the " k_p " calculated is an artifact [123]. An obvious argument against treating this as a "first order rate constant" is that the value of such a "rate constant" is a function of I_i. Furthermore, when [X] is high enough to absorb nearly all the incident light, the rate of the photochemical reaction becomes independent of substrate concentration, that is, it is zero order [X]. *Thus, there is no unimolecular rate constant associated with this process.*

Figure A1 further illustrates this point using actual experimental data. The initial concentration of the substrate X was sufficiently high to give an absorbance of ~2.0 at λ_{irr} so that ~99% of the incident light was absorbed. Continuous photolysis depleted the absorbing substrate to give a product that absorbs little at that wavelength. Initially I_{abs} is nearly constant, thus the rate according to eq. 1 is essentially constant. Eventually X is depleted sufficiently that I_{abs} (and thus the rate) decreases with continued photolysis time and presents a curvature in the latter stages according to eq. A3. This curvature can be approximated as an exponential, since, when Abs(λ_{irr}) << 1, the factor (1-10^{-Abs}) $\cong$ 2.3(Abs) and thus is directly proportional to [X]. Since the precision of most spectrophotometers is optimal at absorbance values < 1, the corresponding concentrations are convenient for study. However, any "rate constant" calculated from such treatment of the data is an artifact of this feature and is misleading.

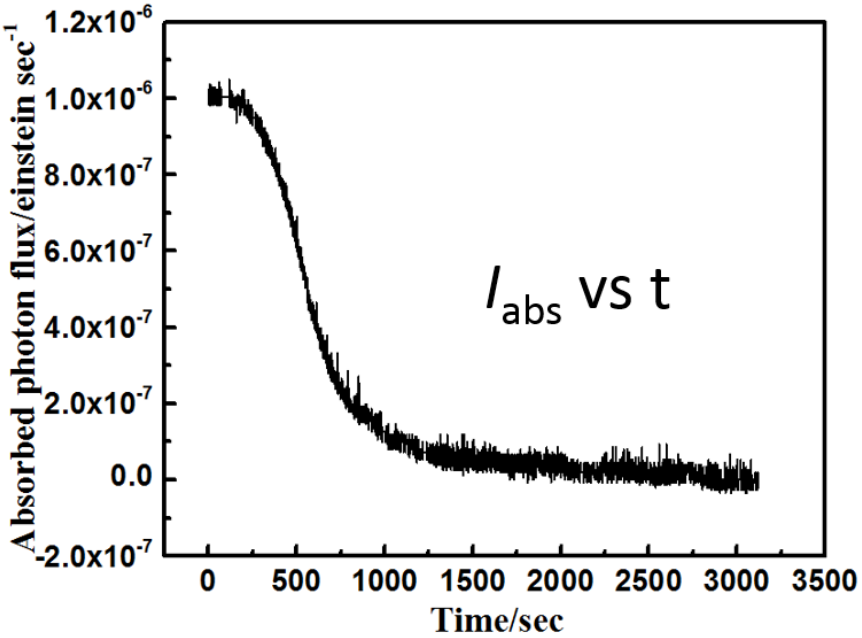

Figure. A1. Changes in the absorbed light intensity (I_{abs}) at the irradiation wavelength as a function of the continuous irradiation time for a photoactive compound measured with a power meter. (Taken with permission from the Ph.D. Dissertation of Zhi Li, University of California, Santa Barbara, 2017)

13. References:

[1] L. J. Ignarro, ed., "Nitric Oxide: Biology and Pathobiology" 2nd Ed. Elsevier Inc., Burlington, MA, 2010.

[2] Biological nitric oxide signaling: chemistry and terminology. T. A. Heinrich, R. S. da Silva, K. M. Miranda, C. H. Switzer, D. A. Wink, J. M. Fukuto, Brit. J. Pharmocol. 169 (2013) 1417-1429.

[3] (a) Nitric oxide release: part II. Therapeutic applications. A. W. Carpenter, M. H. Schoenfisch, Chem. Soc. Rev. 41 (2012) 3742-3752. (b) Nitric Oxide Regulation of Bacterial Biofilms. D. P. Arora, S. Hossain, Y. Xu, E. M. Boon, Biochemistry, 54 (2015) 3717-3728.

[4] Metal complexes as photochemical nitric oxide precursors: Potential applications in the treatment of tumors. A. D. Ostrowski, P. C. Ford, Dalton Transactions., 48 (2009) 10660-10669.

[5] (a) Carbon monoxide – physiology, detection and controlled release. S. H. Heinemann, T. Hoshi, M. Westerhausen, A. Schiller, Chem. Commun. 50 (2014) 3644–3660. (b) Carbon Monoxide and Its Controlled Release: Therapeutic Application, Detection, and Development of Carbon Monoxide Releasing Molecules (CORMs). K. Ling, F. Men, W.-C. Wang, Y.Q. Zhou, H. W. Zhang, D.-W. Ye, J. Med. Chem. 61 (2018) 2611-2635. (c) A manganese photosensitive tricarbonyl molecule [Mn(CO)(3)(tpa-kappa N-3)]Br enhances antibiotic efficacy in a multi-drug-resistant Escherichia coli. N. Rana, H. E. Jesse, M. Tinajero-Trejo, J. A. Butler, J. D. Tarlit, M. L. zur Muhlen, U. Schatzschneider, R. K. Poole, Microbiology, 163 (2017) 1477-1489.

[6] The therapeutic potential of carbon monoxide. R. Motterlini, L. E. Otterbein, Nat. Rev. Drug Discov. 9 (2010) 728–743.

[7] Gasotransmitters in cancer: from pathophysiology to experimental therapy. C. Szabo, Nat. Rev. Drug Discov., 15 (2016) 185-203.

[8] (a) Nitric oxide, a double-edged sword in cancer biology: searching for therapeutic opportunities. S. Mocellin, V. Bronte. D. Nitti, Med. Res. Rev. 27 (2007) 317–352. (b) Cancer cell metabolism and the modulating effects of nitric oxide. C. F. Chang, A. R. Diers, N. Hogg, Free Rad. Biol. Med. 79 (2015) 324-336.

[9] The chemical biology of nitric oxide: Implications in cellular signaling, D. D. Thomas, L. A. Ridnour, J. S. Isenburg, W. Flores-Santana, C. Switzer, S. Donzelli, P. Hussain, C. Vecoli, N. Paolocci, S. Ambs, C. A. Colton, C. C. Harris, D. D. Roberts, D. A. Wink. Free Radical Biol. Med. 45 (2008) 18-31.

[10] (a) “NONOates” (1-substituted diazen-1-ium-1,2-diolates) as nitric oxide donors: Convenient nitric oxide dosage forms. L. K. Keefer, R. W. Nims, K. M. Davies, D. A. Wink, Methods in Enzymology 268 (1996) 281-293. (b) "Nitric Oxide Donors: For Pharmaceutical and Biological Applications" P. G. Wang, T. B. Cai, N. Taniguchi, Ed. Blackwell Science Publishers, Oxford, 2005. (c) Polymers incorporating nitric oxide releasing/generating substances for improved biocompatibility of blood-contacting medical devices M. C. Frost, M. M. Reynolds, M. E. Meyerhoff, Biomaterials, 26 (2005) 1685-1693. (d) Cephalosporin-3 '-diazeniumdiolates: Targeted NO-Donor Prodrugs for Dispersing Bacterial Biofilms. N. Barraud, B. G. Kardak, N. R. Yepuri, R. P. Howlin, J. S. Webb, S. N. Faust, S. Kjelleberg, S. A. Rice, M. J. Kelso, Angew. Chem. Int. Ed. 51 (2012) 9057-60. (e) Nitric Oxide (NO) Releasing Poly ADP-ribose Polymerase 1 (PARP-1) Inhibitors Targeted to Glutathione S-Transferase P1-Overexpressing Cancer Cells. A. E. Maciag, R. Holland, Y. Kim, V. Kumari, C. E. Luthers, W. S. Sehareen, D. Biswas, N. Morris, X. Ji, L. M. Anderson, J. E. Saavedra, L. K. Keefer, J. Med. Chem. 57 (2014) 2292-2302.

[11] Endogenous formation of carbon monoxide in man under normal and pathological conditions. T. Sjostrand, Scand. J. Clin. Lab. Invest. 1 (1949) 201; Also Nature 164 (1949) 580-581.

[12] (a) Developing drug molecules for therapy with carbon monoxide. C. C. Romao, W. A. Blaettler, J. D. Seixas, G. J. L. Bernardes, Chem. Soc. Rev., 41 (2012) 3571-83. (b) Carbon-Monoxide-Releasing Molecules for the Delivery of Therapeutic CO *In Vivo*. S. García-Gallego; G.J.L. Bernardes. Angew. Chem., I. E. 53 (2014) 9712-9721. (c) Novel lead structures and activation mechanisms for CO-releasing molecules (CORMs). U. Schatzschneider, Brit. J. Pharmacology 172 (2015) 1638-1650. (d) Nonmetallic carbon monoxide releasing molecules (CORMs). N Abeyrathna, K. Washington, C. Bashur, Y. Liao, Organic & Biomolecular Chem. 15 (2017) 8692-8699.

[13] Cardioprotective actions by a water-soluble carbon monoxide-releasing molecule. J. E. Clark, P. Naughton, S. Shurey, C. J. Green, T. R. Johnson, B. E. Mann, R. Foresti, R. Motterlini, Circulation Res. 93 (2013) E2-E8.

[14] Keys for Unlocking Photolabile Metal-Containing Cages. K. L. Ciesienski, K. J. Franz. Angew. Chem. Int. Ed. 50 (2011) 814-824.

[15] A Visible-Light-Sensitive Caged Serotonin, R. Cabrera, O. Filevich, B. Garcia-Acosta, J. Athilingam, K. J. Bender, K. E. Poskanzer, R. Etchenique, ACS Chem. Neurosci. 8 (2017) 1036-1042.

[16] Light Activation of a Cysteine Protease Inhibitor: Caging of a Peptidomimetic Nitrile with Ru-II(bpy). T. Respondek, R. N. Garner, M. K. Herroon, I. Podgorski, C. Turro, J. J. Kodanko, J. Am. Chem. Soc. 133 (2011) 17164-17167.

[17] (a) Chemical radiosensitizers for use in radiotherapy, P. Wardman, Clincal Oncology, 19 (2007) 397-417. (b) The impact of hypoxia and its modification of the outcome of radiotherapy, M. R. Horsman, J. Overgaard, J. Rad. Res. 57 (2016), 190-198

[18] (a) Hypoxic Mammalian Cell Radiosensitization by Nitric Oxide. J. B. Mitchell, D. A. Wink, W. DeGraff, J. Gamson, L. Keefer, M. C. Krishna, Cancer Res. 33 (1993) 5845-8. (b) Nitric oxide as a radiosensitizer: Evidence for an intrinsic role in addition to its effect on oxygen delivery and consumption. B. F. Jordan, P. Sonveaux, O. Feron, V. Gregoire, N. Beghein, C. Dessy, B. Gallez, Internl. J. Cancer 109 (2004) 768-773.

[19] New insight into the functioning of nitric oxide receptive guanylyl cyclase: physiological and pharmacological implications. J. Garthwaite, Mol. Cell. Biochem. 334 (2010) 221-232.

[20] Photochemistry of Roussin's red salt and of Roussin's black salt In situ nitric oxide generation to sensitize gamma-radiation induced cell death. J. Bourassa, W. DeGraff, S. Kudo, D. A. Wink, J. B. Mitchell, P. C. Ford, J. Am. Chem. Soc. 119 (1997) 2853-2862.

[21] Nitric Oxide and Ionizing Radiation Synergistically Promote Apoptosis and Growth Inhibition of Cancer by Activating p53. T. Cook, Z. Wang, S. Alber, K. Liu, S. C. Watkins, V. Vodovotz, T. R. Billiar, D. Blumberg, Cancer Res. 64 (2014) 8015-8021.

[22] Photochemistry of metal nitrosyl complexes. Delivery of nitric oxide to biological targets. P. C. Ford, J. Bourassa, K. M. Miranda, B. Lee, I. Lorkovic, S. Boggs, S. Kudo, L. Laverman. Coord. Chem. Rev. 171 (1998) 185-202.

[23] (a) Photoreactivity of the ruthenium nitrosyl complex, Ru(salen)(Cl)(NO). Solvent effects on the back reaction of NO with the Lewis acid Ru^{III}(salen)(Cl). C. F. Works, P. C. Ford, *J. Am. Chem. Soc. 122* (2000) 7592–7593. (b) Photochemical nitric oxide precursors: Synthesis, photochemistry and ligand substitution kinetics of ruthenium salen nitrosyl and ruthenium salophen nitrosyl complexes. C. F. Works, C. J. Jocher, G. D. Bart, X. Bu, P.C. Ford, *Inorg. Chem.* 41 (2002) 3728–3739.

[24] Photochemical Production of Nitric Oxide via Two Photon Excitation with NIR Light. S. R. Wecksler, A. Mikhailovsky, P. C. Ford, J. Amer. Chem. Soc. 126 (2004) 13566-13567.

[25] Chromium(III) complexes for photochemical nitric oxide generation from coordinated nitrite. The

synthesis and photochemistry of macrocyclic complexes with pendant chromophores, trans-$[Cr(L)(ONO)_2]BF_4$, F. DeRosa, X. Bu, P. C. Ford, Inorg. Chem 44 (2005) 4157-65.

[26] (a) Photosensitized NO Release from Water Soluble Nanoparticle Assemblies, D. Neuman, A.D. Ostrowski, R. O. Absalonson, G. F. Strouse, P. C. Ford, J. Am. Chem. Soc. 129 (2007) 4146 – 4147. (b) Quantum Dot Fluorescence Quenching Pathways of Electrostatic Assemblies with Cr(III) Complexes. Sensitized Nitric Oxide Production from trans-$Cr(cyclam)(ONO)_2^+$. D. Neuman, A. D. Ostrowski, A. A. Mikhailovsky, R. Absalonson, G. F. Strouse, P. C. Ford, J. Amer. Chem. Soc. 130 (2008) 68-75.

[27] Polychromophoric Metal Complexes for Generating the Bioregulatory Agent Nitric Oxide by Single and Two Photon Excitation, P. C. Ford, Accts. Chem. Res., 41 (2008) 190-200.

[28] (a) Reversible Photolabilization of NO from Chromium(III) Coordinated Nitrite. A New Strategy for Nitric Oxide Delivery. M. A. De Leo, P. C. Ford *J. Am. Chem. Soc. 121* (1999) 1980-1981. (b)The Photochemistry of trans-$Cr(cyclam)(ONO)_2^+$, a Nitric Oxide Precursor. A. D. Ostrowski, R. O. Absalonson, M. A. De Leo, G. Wu, J. G. Pavlovich, J. Adamson, B. Azhar, A. V. Iretskii, I. L. Megson, P. C. Ford, Inorg. Chem., 50 (2011) 4453-4462. (Correction: Inorg. Chem. 50 (2011) 5848.) (c) Nitric Oxide Photogeneration from trans-$Cr(cyclam)(ONO)_2^+$ in a Reducing Environment. Activation of Soluble Guanylyl Cyclase and Arterial Vasorelaxation. Alexis. D. Ostrowski, S. J. Deakin, B. Azhar, T. W. Miller, N. Franco, M. M. Cherney, A. J. Lee, J. N. Burstyn, J. M. Fukuto, I. L. Megson, P. C. Ford, J. Med. Chem., 53 (2010) 715-722.

[29] Near-Infrared Triggered Release of Caged Nitric Oxide using Upconversion Nanostructured Materials. J. V. Garcia, J. Yang, D. Shen, C. Yao, X. Li, G. D. Stucky, D. Zhao, P. C. Ford, F. Zhang. Small 8 (2012) 3800–3805.

[30] Nitric Oxide Releasing Materials Triggered by Near-Infrared Excitation Through Tissue Filters, P. T. Burks, J. V. Garcia, R. GonzalezIrias, J. T. Tillman, M. Niu, J. Zhang, F. Zhang, P. C. Ford, J. Am. Chem. Soc. 135 (2013) 18145-18152.

[31] Photochemical delivery of nitric oxide. P. C. Ford, Nitric Oxide 34 (2013) 56-64.

[32] Near-IR mediated intracellular uncaging of nitric oxide from cell-targeted hollow gold nanoparticles. E. S. Levy, D. P. Morales, J. V. Garcia, N. O. Reich, P. C. Ford, Chem. Commun. 51 (2015) 17692-17695.

[33] Macrophage-Mediated Delivery of Light Activated Nitric Oxide Prodrugs with Spatial, Temporal and Concentration Control. M. Evans, P. J. Huang, Y. Iwamoto, K. Ibsen, E. Chan, Y. Hitomi, P. C. Ford, S. Mitragotri, Chemical Science, 9 (2018) 3729-3741.

[34] (a) Structure, chemical and photochemical reactivity and biological activity of some ruthenium amine nitrosyl complexes. E. Tfouni, M. Krieger, B. R. McGarvey, D. W. Franco, Coord. Chem. Rev. 236 (2003) 57-69. (b) Light-triggered and cysteine-mediated nitric oxide release from a biodegradable starch-based film. A. C. Roveda, H. Aguiar, K. M. Miranda, C. C. Tadini, D. W. Franco, J. Mat. Chem B, 2 (2014) 7232-7242. (c) Tailoring NO Donors Metallopharmaceuticals: Ruthenium Nitrosyl Ammines and Aliphatic Tetraazamacrocycles. E. Tfouni, F.G. Doro, L.E. Figueiredo, J.M.C. Pereira, G. Metzker, D.W. Franco, Curr. Med. Chem. 17 (2010) 3643-3657. (d) trans-[Ru(NO)Cl(cyclam)](PF6)(2) and [Ru(NO)(Hedta)] Incorporated in PLGA Nanoparticles for the Delivery of Nitric Oxide to B16-F10 Cells: Cytotoxicity and Phototoxicity. A. J. Gomes, E. M. Espreafico, E. Tfouni, Mol. Pharmaceutics 10 (2013) 3544-3554.

[35] Photosensitive Precursors to Nitric Oxide. C. M. Pavlos, H. Xu, J. P. Toscano, Cur. Topics Med. Chem. 5 (2005) 635-647.

[36] (a) Photoactive ruthenium nitrosyls: Effects of light and potential application as NO donors, M. J. Rose, P. K. Mascharak, Coord. Chem. Rev. 252 (2008) 2093-2114. (b) Light-triggered nitric oxide delivery to malignant sites and infection, B. Heilman, P. K. Mascharak, Phil. Trans. Roy. Soc. A. 371(1995) (2013), Article No: 20120368. (c) Recent Progress in Photoinduced NO Delivery With

Designed Ruthenium Nitrosyl Complexes. T. R. deBoer, P. K. Mascharak, Adv. Inorg. Chem. 67 (2015) 145-170.

[37] (a) Light-controlled nitric oxide delivering molecular assemblies. S. Sortino, Chem. Soc. Rev. 39 (2010) 2903-2913. (b) Photoactivated nanomaterials for biomedical release applications, S. Sortino, J. Mat. Chem. 22 (2012) 301-318. (c) Photoactivable Platforms for Nitric Oxide Delivery with Fluorescence Imaging, A. Fraix, S. Sortino, Chemistry-An Asian J. 10 (2015) 1116-1125. (d) Phototherapeutic Release of Nitric Oxide with Engineered Nanoconstructs. A. Fraix, N. Marino, S. Sortino, Top. Curr. Chem. 370 (2016) 225–258. (e) Monitoring the release of a NO photodonor from polymer nanoparticles via Forster resonance energy transfer and two-photon fluorescence imaging. C. Conte, A. Fraix, H. Thomsen, F. Ungaro, V. Cardile, A. C. E. Graziano, M. B. Ericson, F. Quaglia, S. Sortino, J. Mat. Chem. B, 6 (2018) 249-256. (f) Photoinduced Fluorescence Activation and Nitric Oxide Release with Biocompatible Polymer Nanoparticles. E. Deniz, N. Kandoth, A. Fraix, V. Cardile. A. C. E. Graziano, D. Lo Furno, R. Gref, F. M. Raymo, S. Sortino, Chem. Eur. J. 18 (2012) 15782–15787.

[38] Synthesis, spectroscopic analysis and photolabilization of water-soluble ruthenium(III)-nitrosyl complexes A. C. Merkle, A. B. McQuarters, N. Lehnert. Dalton Trans. 41 (2012) 8047-8059.

[39] Photomanipulation of Vasodilation with a Blue-Light-Controllable Nitric Oxide Releaser. N. Ieda, Y Hotta, N. Miyata, K. Kimura, H. Nakagawa. J. Am. Chem. Soc. 136 (2014) 7085-7091.

[40] (a) Photoinduced NO release by visible light irradiation from pyrazine-bridged nitrosyl ruthenium complexes. M. G. Sauaia, R. G. de Lima, A. C. Tedesco, R. S. da Silva, J. Am. Chem. Soc. 125 (2003) 14718-14719. (b) Cytosolic calcium concentration is reduced by photolysis of a nitrosyl ruthenium complex in vascular smooth muscle cells. C. N. Lunardi, A. L. Cacciari, R. Santana da Silva, L. N. Bendhack, Nitric Oxide-Biology and Chemistry, 15 (2006) 252-258. (c) Enhanced Antitumor Activity against Melanoma Cancer Cells by Nitric Oxide Release and Photosensitized Generation of Singlet Oxygen from Ruthenium Complexes L. C. B Ramos, M. S. P. Pereira; D. Callejon, M. Baruffi, C. N. Lunardi, L. D. Slep, L. M. Bendhack, R. S. da Silva, Europ. J. Inorg. Chem. 22 (2016) 3592-3597.

[41] Light-controlled release of nitric oxide from solid polymer composite materials using visible and near infra-red light. J. D. Mase, A. O. Razgoniaev, M. K. Tschirhart, A. D. Ostrowski, PhotoChem. Photobiol. Sci. 14 (2015) 777-785..

[42] Nitric Oxide: A Key Mediator of Biofilm Dispersal with Applications in Infectious Diseases. N. Barraud, M. J. Kelso, S. A. Rice, S. Kjelleberg, Current Pharmaceutical Design,) 21 (2015) 31-42. Accession Number: WOS:000345434600006.

[43] A two-photon excitable and ratiometric fluorogenic nitric oxide photoreleaser and its biological applications. X. Xie, J. Fan, M. W. Liang, Y. Li, X. Jiao, B. Wang, Chem. Commun. 53, (2017) 11941-11944.

[44] A Photochemical Precursor for Carbon Monoxide Release in Aerated Aqueous Solution R. Dale Rimmer, H. Richter, P C. Ford, Inorg. Chem. 49 (2010) 1180-1185.

[45] Photochemically Activated Carbon Monoxide Release for Biological Targets. Developing Air-Stable Group 6 PhotoCORMs Labilized by Visible Light. R. D. Rimmer, A. E. Pierri, P. C. Ford, Coord. Chem. Rev. 256 (2012) 1509-1519.

[46] PhotoCORM nanocarrier for CO release using NIR light. A. Pierri, P.-J. Huang, J. V. Garcia, J. Stanfill, M. Chui, N. Zheng, P. C. Ford, Chem. Commun. 51 (2015) 2072-2075.

[47] Dinuclear PhotoCORMs: Dioxygen-Assisted Carbon Monoxide Uncaging from Long-Wavelength - Absorbing Metal-Metal-Bonded Carbonyl Complexes. Z. Li, A. E. Pierri, P. J. Huang, G. Wu, P. C. Ford. Inorg. Chem. 56 (2017) 6094-6104. (Correction: Inorg. Chem. 57 (2018) 6191.)

[48] Photoactivated *in Vitro* Anticancer Activity of Rhenium(I) Tricarbonyl Complexes Bearing Water-Soluble Phosphines. S. C. Marker, S. M. MacMillan, W. R. Zipfel, Z. Li, P. C. Ford, J. J. Wilson, Inorg. Chem. 57 (2018) 1311-1331.

[49] (a) Photoinduced CO release, cellular uptake and cytotoxicity of a tris(pyrazolyl)methane (tpm) manganese tricarbonyl complex. J. Niesel, A. Pinto, H. W. Peindy N'dongo, K. Merz, I. Ott, R. Gust, U. Schatzschneider, Chem. Commun. (2008) 1798–1800. (b) Photoactivated Biological Activity of Transition-Metal Complexes. U. Schatzschneider, Europ. J. Inorg. Chem. 10 (2010) 1451-1467. (c) PhotoCORMs: Light-triggered release of carbon monoxide from the coordination sphere of transition metal complexes for biological applications. U. Schatzschneider, Inorg. Chim. Acta, 374 (2011) 19-23. (d) Next Generation PhotoCORMs: Polynuclear Tricarbonylmanganese(I)-Functionalized Polypyridyl Metallodendrimers. P. Govender, S. Pai, U. Schatzschneider, G. Smith, Inorg. Chem. 52 (2013) 5470-5478.

[50] The chemistry, biology and design of photochemical CO releasing molecules and the efforts to detect CO for biological applications. J. Marhenke, K. Trevino, C. F. Works, Coord. Chem. Rev. 306 (2016) 533-543.

[51] (a) A Theranostic Two-Tone Luminescent PhotoCORM Derived from Re(I) and (2-Pyridyl)-benzothiazole: Trackable CO Delivery to Malignant Cells. S. J. Carrington, I. Chakraborty, J. M. L. Bernard, P. K. Mascharak, Inorg. Chem. 55 (2016) 7852-7858. (b) Eradication of HT-29 colorectal adenocarcinoma cells by controlled photorelease of CO from a CO-releasing polymer (photoCORP-1) triggered by visible light through an optical fiber-based device. M. N. Pinto, I. Chakraborty, C. Sandoval, P. K. Mascharak, J. Control. Release 274 (2017) 192-202. (c) A Luminescent Manganese PhotoCORM for CO Delivery to Cellular Targets under the Control of Visible Light. J. Jimenez, I. Chakraborty, A. Dominguez, J. Martinez-Gonzalez, W. M. C. Sameera, W. M. Chamil, P. K. Mascharak, Inorg. Chem. 57 (2018) 1766-1773

[52] (a) Properties of a flavonol-based photoCORM in aqueous buffered solutions: influence of metal ions, surfactants and proteins on visible light-induced CO release. M. Popova, T. Soboleva, A. M. Arif, L. M. Berreau, RSC Advances 7 (2017) 21997-22007. (b) Sense and Release: A Thiol-Responsive Flavonol-Based Photonically Driven Carbon Monoxide-Releasing Molecule That Operates via a Multiple-Input AND Logic Gate. T. Soboleva, H. J. Esquer, A. D. Benninghoff, L. M. Berreau, J. Amer. Chem. Soc. 139 (2017) 9435-9438. (c) Transition-Metal-Free CO-Releasing BODIPY Derivatives Activatable by Visible to NIR Light as Promising Bioactive Molecules. E. Palao, T. Slanina, L. Muchova, T. Solomek, L. Vitek, P. Klan, J. Am.Chem. Soc. 138 (2016) 126−133.

[53] (a) Red Light-Triggered CO Release from Mn2(CO)(10) Using Triplet Sensitization in Polymer Nonwoven Fabrics. S. H. C. Askes, G. Reddy, W. Upendar; S. Bonnet, A. Schiller, J. Am. Chem. Soc. 139 (2017) 15292-15295. (b) Manganese(I)-Based CORMs with 5-Substituted 3-(2-Pyridyl)Pyrazole Ligands. R. Mede, S. Glaeser, B. Suchland, B. Schowtka, M. Mandel, H. Goerls, S. Krieck, A. Schiller, M. Westerhausen, Inorganics 5 (2017) article 8. (c) Precision gas therapy using intelligent nanomedicine. Q. He, BioMatarials Sci., 5 (2017) 2226-2230.

[54] (a)Mechanism of NO Photodissociation in Photo labile Manganese-NO Complexes with Pentadentate N5 Ligands. A. C. Merkle, N. L. Fry, P. K. Mascharak, N. Lehnert, Inorg. Chem. 50 (2011) 12192-12203. (b) Electronic Tuning of Nitric Oxide Release from Manganese Nitrosyl Complexes by Visible Light Irradiation: Enhancement of Nitric Oxide Release Efficiency by the Nitro-Substituted Quinoline Ligand. Y. Hitomi, Y. Iwamoto, M. Kodera, Dalton Trans. 43 (2013) 2161–2167. (c) Uncaging a catalytic hydrogen peroxide generator through the photo-induced release of nitric oxide from a {MnNO}(6) complex. Y. Iwamoto, M. Kodera, Y. Hitomi, Chem. Commun. 51 (2015) 9539-9542.

[55] (a) Photo-controlled release of NO and CO with inorganic and organometallic complexes. A. E. Pierri,

D. A. Muizzi, A. D. Ostrowski, P. C. Ford, Structure & Bonding 165 (2015) 1-45. (b) PhotoCORMs: CO release moves into the visible. M. A. Wright, J. A. Wright, Dalton Trans. 45 (2016) 6801-6811. (c) Visible Light-Activated PhotoCORMs, E. Kottelat, F. Zobi, Inorganics 5 (2017) 24. (d) Transition-Metal Nitrosyls for Photocontrolled Nitric Oxide Delivery. H.-J. Xiang, M. Guo, J.-G. Liu, Eur. J. Inorg. Chem. (2017) 1586–1595.

[56] (a) Konig, K. Multiphoton microscopy in life sciences. J. Microscopy, 2000, 200, 83-104. (b) Bioimaging. Second window for *in vivo* imaging. A. M. Smith, M. C. Mancini, S. Nie, Nature Nanotech. 4 (2009) 710-711.

[57] (a) Novel nitric oxide generating compound glycidyl nitrate enhances the therapeutic efficacy of chemotherapy and radiotherapy S. Ning, M. Bednarski, B. Oronsky, J. Scicinski, S. J. Knox, Biochem Biophys. Res. Comm. 447 (2014) 537-542. (b) Nitric oxide: role in tumour biology and iNOS/NO-based anticancer therapies. S. Singh, A. K. Gupta, Cancer Chemotherapy and Pharmacology, 67 (2001) 1211-1224.

[58] The biological lifetime of nitric oxide: Implications for the perivascular dynamics of NO and O2, D. D. Thomas, Z. P Liu, S. P. Kantrow, J. R. Lancaster, Proc. Nat. Acad. Sci. (USA) 98 (2001) 355-360.

[59] Determination of the Carbon Monoxide Binding Constants of Myoglobin Mutants: Comparison of Kinetic and Equilibrium Methods. S. Balasubramanian, D. G. Lambright, J. H. Simmons, S. J. Gill, S. G. Boxer, Biochemistry, 33 (1994)8355-8360

[60] Chromium(III) complexes for photochemical nitric oxide generation from coordinated nitrite. The synthesis and photochemistry of macrocyclic complexes with pendant chromophores, trans-$[Cr(L)(ONO)_2]BF_4$, F. DeRosa, X. Bu, P. C. Ford, Inorg. Chem. 44 (2005) 4157-65.

[61] Synthesis and Photochemical Properties of a Novel Protoporphyrin IX Derivatized Iron-Sulfur-Nitrosyl Cluster, C. L. Conrado, S. Wecksler, C. Egler, D. Magde, P. C. Ford, Inorg. Chem. 43 (2004) 5543-5549.

[62] A Two-Photon Antenna for Photochemical Delivery of Nitric Oxide from a Water Soluble, Dye Derivatized Iron Nitrosyl Complex Using NIR Light, S. R. Wecksler, A. Mikhailovsky, D. Korystov, P. C. Ford, J. Amer. Chem. Soc., 128 (2006) 3831-3837.

[63] Liposome encapsulation of a photochemical NO precursor for controlled nitric oxide release and simultaneous fluorescence imaging, A. D. Ostrowski, B. F. Lin, M. V. Tirrell, P. C. Ford, Molecular Pharmaceuticals 9 (2012) 2950-2955.

[64] Photochemistry of Metal Carbonyls. M. S. Wrighton, Chem. Rev. 74 (1974) 401–30.

[65] (a) Photochemical Strategies for Investigating Organometallic Intermediates Relevant to Catalysis Mechanisms. P. C. Ford, J. S. Bridgewater, S. Massick, J. Marhenke, Catalysis Today, 49 (1999) 419-430. (b) Time Resolved Spectroscopic Studies Relevant to Reactive Intermediates in Homogeneous Catalysis. P. C. Ford, S. Massick, Coord. Chem. Rev. 226 (2002) 39–49.

[66] (a) Carbon Monoxide-Releasing Molecules. R. Motterlini, J. E. Clark, R. Foresti, P. Sarathchandra, B. E. Mann, C. Green, C. J. Circulation Res. 90 (2002) e17–e24. (b) Acute renal hemodynamic effects of dimanganese decacarbonyl and cobalt protoporphyrin. B. A. Arregui, B. L. Pez, M. Garca Salom, F. Valero, C. N. Navarro, F. J. Fenoy, Kidney Int. 65 (2004) 564–574. (c) The permissive role of endothelial NO in CO-induced cerebrovascular dilation E. Barkoudah, J. H. Jaggar, C. W. Leffler, Am. J. Physiol.: Heart Circ. Physiol. 87 (2004) H1459–H1465.

[67] Modification of the deoxy-myoglobin/carbonmonoxy-myoglobin UV-vis assay for reliable determination of CO-release rates from organometallic carbonyl complexes. A. J. Atkin, J. M. Lynam, B. R. Moulton, P. Sawle, R. Motterlini, N. M. Boyle, M. T. Pryce, I. J. S. Fairlamb, Dalton Trans. 40 (2011) 5755-5761.

[68] Photosubstitution reactivity of a series of pentacarbonylpyridinetungsten(0) complexes having ligand-field or charge transfer lowest excited states. M. S. Wrighton, H. B. Abrahamson, D. L Morse. J. Amer. Chem. Soc. 98 (1976) 4105-4109.

[69] Mechanistic interpretation of high-pressure effects on the photosubstitution of pyridine and 4-substituted pyridine in complexes of tungsten pentacarbonyl. S. Wieland, R. van Eldik, D. R. Crane, P. C. Ford, Inorg. Chem. 28 (1989) 3663.

[70] A Luminescent and Biocompatible PhotoCORM. A. E. Pierri, A. Pallaoro, G. Wu, P. C. Ford, J. Amer. Chem. Soc. 134 (2012) 18197-18200. (correction: J. Amer. Chem. Soc. 140 (2018), 525.)

[71] (a) Red-light activated photo-CORMs of Mn(I) species bearing electron deficient 2,2′-azopyridines. E. Kottelat, A. Ruggi, F. Zobi, Dalton Trans. 45 (2016) 6920–6927. (b) Rapid green and blue light-induced CO release from bromazepam Mn(I) and Ru(II) carbonyls: synthesis, density functional theory and biological activity evaluation. A. M. Mansour, Appl. Organomet. Chem. 31 (2017) e3564.

[72] Photodynamic Therapy - Two photons are better than one. S. Brown, Nature Photonics 2 (2008) 394-395.

[73] A Two-Photon Antenna for Photochemical Delivery of Nitric Oxide from a Water Soluble, Dye Derivatized Iron Nitrosyl Complex Using NIR Light, S. R. Wecksler, A. Mikhailovsky, D. Korystov, P. C. Ford, J. Amer. Chem. Soc., 128 (2006) 3831-7.

[74] (a) Single and two photon properties of a dye derivatized Roussin's red salt ester with a large TPA cross section, S. R. Wecksler, A. Mikhailovsky, D. Korystov, F. Buller, R. Kannan, L.-S. Tan, P. C. Ford. Inorg. Chem. 46 (2007) 395-402. b) Water-Soluble Two-Photon Absorbing Nitrosyl Complex for Light Activated Therapy Through Nitric Oxide Release, Q. Zheng, A. Bonoiu, T. Y. Ohulchanskyy, G. S. He, P. N. Prasad, Mol. Pharm. *5* (2008) 389-398.

[75] (a) Photoinduced Nitric Oxide Release from a Hindered Nitrobenzene Derivative by Two-Photon Excitation. K. Hishikawa, H. Nakagawa, T. Furuta, K. Fukuhara, H. Tsumoto, T. Suzuki, N. Miyata, J. Am. Chem. Soc. 131 (2009) 7488. (b) A double bond-conjugated dimethylnitrobenzene-type photolabile nitric oxide donor with improved two-photon cross section. N. Ieda, K. Hishikawa, K. Eto, K. Kitamura, M. Kawaguchi, T. Suzuki, K. Fukuhara, N Miyata, T. Furuta, J. Nabekura, H. Nakagawa, Bioorg. Med. Chem. Let. 25 (2015) 3172-3175.

[76] Nitric oxide release triggered by two-photon excited photoluminescence of engineered nanomaterials. L. Tan, A. Wan, X. Zhu, H. Li, Chem. Commun. 50 (2014) 5725-5728.

[77] Rational Design of a Robust Fluorescent Probe for the Detection of Endogenous Carbon Monoxide in Living Zebrafish Embryos and Mouse Tissue. K. Liu, X. Kong, Y. Ma, W. Lin, Angew. Chem. Int. Ed. 56 (2017) 13489-13492

[78] Photoreactivity of a Quantum Dot-Ruthenium Nitrosyl Conjugate. L. P. Franco, S. A. Cicillini, J. C. Biazzotto, M. A. Schiavon, A. Mikhailovsky, P. Burks, J. V. Garcia, P. C. Ford, R. S. da Silva, J. Phys. Chem. A 118 (2014) 12184-12191.

[79] Quantum Dot Photosensitizers. Interactions with Transition Metal Centers, P. T. Burks, P. C. Ford, Dalton Trans. 41 (2012) 13030-42.

[80] (a) Luminescent quantum dots as platforms for probing *in vitro* and *in vivo* biological processes, H. Mattoussi, G. Palui, H. Bin Na, Adv. Drug. Delivery Rev. 2012, 64 138-166. (b) Semiconductor quantum dots as two-photon sensitizers, S. Dayal, C. Burda, J. Am. Chem. Soc. 130 (2008) 2890-2891.

[81] Quantum Dot Photoluminescence Quenching by Cr(III) Complexes. Photosensitized Reactions and Evidence for a FRET Mechanism. P. T. Burks, A. D. Ostrowski, A. A. Mikhailovsky, E. M. Chan, P. S. Wagenknecht, P. C. Ford, J. Am. Chem. Soc. 134 (2012) 13266-13275.

[82] Photocatalytic carbon disulfide production via charge transfer quenching of quantum dots. Chris M. Bernt, P.T. Burks, A. W. DeMartino, A. E. Pierri, E. S. Levy, D. F. Zigler, P. C. Ford. J. Am. Chem. Soc. 136 (2014) 2192-2195.

[83] (a) Ag_2S Quantum Dots Conjugated Chitosan Nanospheres toward Light-Triggered Nitric Oxide Release and Near-Infrared Fluorescence Imaging. L. Tan, A. Wan, H. Li, Langmuir 29 (2013) 15032-15042. (b) Conjugating S-Nitrosothiols with Glutathiose Stabilized Silver Sulfide Quantum Dots for Controlled Nitric Oxide Release and Near-Infrared Fluorescence Imaging. L. Tan, A. Wan, H. Li, ACS Appl. Mater. Interfaces 5 (2013) 11163-11171.

[84] Kinetics studies of the reaction of the ruthenium porphyrin Ru(OEP)(CO) with the *S*-nitrosothiol *N*-Acetyl-1-amino-2-methylpropyl-2-thionitrite. L. V. Andreasen, I. M. Lorkovic, G. B. Richter-Addo, P.C. Ford, Nitric Oxide: Chemistry and Biology 6 (2002) 228-235.

[85] Carbon quantum dot photoreleaser nanohybrids for two-photon phototherapy of hypoxic tumors. C. Fowley, A. P. McHale, B. McCaughan, A. Fraix, S. Sortino, J. F. Callan, Chem. Commun. 51 (2015) 81-84.

[86] Ruthenium nitrosyl functionalized graphene quantum dots as an efficient nanoplatform for NIR-light-controlled and mitochondria-targeted delivery of nitric oxide combined with photothermal therapy. M. Guo, H.-J. Xiang, Y. Wang, Q.-L. Zhang, L. An, S.-P. Yang, Y. Ma, Y. Wang, J.-G. Liu, Chem. Commun. 53 (2017) 3253-3256.

[87] A ruthenium-nitrosyl-functionalized nanoplatform for the targeting of liver cancer cells and NIR-light-controlled delivery of nitric oxide combined with photothermal therapy. Y.-H. Li, M. Guo, S.-W. Shi, Q.-L. Zhang, S.-P. Yang, J.-G. Liu**,** *J. Mater. Chem. B,* 5 (2017) 7831-7838.

[88] Ph.D. Dissertation of Po-Ju Huang, University of California, Santa Barbara (2017)

[89] A Brief Introduction to Cell-Penetrating Peptides. P. Lundberg, Ü. Langel, J. Mol. Recognit. 16 (2003) 227–233.

[90] Quantum-CORMs: quantum dot sensitized CO releasing molecules. A. Ruggi, F. Zobi, Dalton Trans. 44 (2015) 10928-10931.

[91] Macromolecular and Inorganic Nanomaterials Scaffolds for Carbon Monoxide Delivery: Recent Developments and Future Trends. D. Nguyen, C. Boyer, ACS Biomat. Sci. Eng. 1 (2015) 895-913.

(92) Encapsulation of a nitric oxide donor into a liposome to boost the enhanced permeation and retention (EPR) effect. Y.Tahara, T. Yoshikawa, H. Sato, Y. Mori, M. H. Zahangir, A. Kishimura, T.i Mori, Y. Katayama, Med. Chem. Commun. 8 (2017) 415-421

(93) Lipophilic ruthenium salen complexes: incorporation into liposome bilayers and photoinduced release of nitric oxide. K. Nakanishi, T. Koshiyama, S. Iba, M. Ohba, Dalton Trans. 44 (2015) 14200-14203

[94] (a) Noble Metals on the Nanoscale: Optical and Photothermal Properties and Some Applications in Imaging, Sensing, Biology, and Medicine. P. K. Jain, X. Huang, I. H. El-Sayed, M. A. El-Sayed, Accts. Chem. Res. 41 (2008) 1578-1586. (b) Biodistribution and toxicity of engineered gold nanoparticles: a review of *in vitro* and *in vivo* studies. N. Khlebtsov, L. Dykman, Chem. Soc. Rev. 40 (2011) 1647-1671.

[95] Nitric oxide photocaging platinum nanoparticles with anticancer potential. M. Barone, M. T. Sciortino, D. Zaccaria, A. Mazzaglia, S. Sortino, J. Mater. Chem. 18 (2008) 5531-5536.

[96] Layer-by-layer assembled gold nanoparticles with a tunable payload of a nitric oxide photocage. P. Taladriz-Blanco, J. Pérez-Juste, N. Kandoth, P. Hervés, S. Sortino, J. of Colloid Interface Sci. 407 (2013) 524-528.

[97] Self-assembled monolayers of thiols and dithiols on gold: new challenges for a well-known system. C. Vericat, M. E. Vela, G. Benitez, P. Carro and R. C. Salvarezza, Chem. Soc. Rev. 39 (2010) 1805–1834.

[98] Tissue-Penetrating Delivery of Compounds and Nanoparticles into Tumors**.** K. N. Sugahara, T. Teesalu, P. P. Karmali, V. R. Kotamraju, L. Agemy, O. M. Girard, D. Hanahan, R. F. Mattrey and E. Ruoslahti, Cancer Cell 16 (2009) 510–520.

[99] (a) Stabilizing Alginate Confinement and Polymer Coating of CO-Releasing Molecules Supported on

Iron Oxide Nanoparticles To Trigger the CO Release by Magnetic Heating. H. Meyer, F. Winkler, P. C. Kunz, A. M. Schmidt, A. Hamacher, M. U. Kassack, C. Janiak , Inorg. Chem. 54 (2015) 11236-11246. (b) Synthesis of oxime-based CO-releasing molecules, CORMs and their immobilization on maghemite nanoparticles for magnetic-field induced CO release. H. Meyer, M. Brenner, S. P. Hoefert, T. O. Knedel, P. C. Kunz, A. M. Schmidt, A. Hamacher, M. U. Kassack, C. Janiak, Dalton Trans, 45 (2016) 7605-76015.

[100] Light responsive metal-organic frameworks as controllable CO-releasing cell culture substrates. S. Diring, A. Carne-Sanchez, J. C. Zhang, S. Ikemura, C. Kim, H. Inaba, S. Kitagawa, S. Furukawa, Chem. Sci. 8 (2017) 2381-2386.

[101] A Reaction-Based Fluorescent Probe for Selective Imaging of Carbon Monoxide in Living Cells Using a Palladium-Mediated Carbonylation B. W. Michel, A. R. Lippert and C. J. Chang, J. Am. Chem. Soc. 134 (2012) 15668-15671.

(102) Nitric oxide-releasing silica nanoparticles with varied surface hydrophobicity. A. W. Carpenter, J. A. Johnson, M. H. Schoenfisch, Colloids Surfaces A: Physicochem. Eng. Aspects, 454 (2014) 144-151.

(103) Delivering nitric oxide with nanoparticles. J. F. Wuinn, M. R. Whittaker, T. P. Davis, J. Controlled Release 2015 (2015) 190-205.

(104) Multivalent mesoporous silica nanoparticles photo-delivering nitric oxide with carbon dots as fluorescence reporters. D. Afonso, S. Valetti, A. Fraix, C. Bascetta, S. Petralia, S. Conoci, A. Feiler, S. Sortino, Nanoscale 9 (2107) 13404- 13408.

(105) Rapid Eradication of Human Breast Cancer Cells through Trackable Light-Triggered CO Delivery by Mesoporous Silica Nanoparticles Packed with a Designed photoCORM. I. Chakraborty, S. J. Carrington, J. Hauser, S. R. J. Oliver, P. K. Mascharak, Chem. Mater. 27 (2015) 8387−8397.

[106] (a) Upconversion nanoparticles in biological labeling, imaging, and therapy. F. Wang, D. Banerjee, Y. Liu, X. Y. Chen, X. G. Liu, Analyst 135 (2010) 1839-1854. (b) Controlling upconversion nanocrystals for emerging applications. B. Zhou, B. Shi, D. Jin, X. G. Liu, Nat. Nanotech. 10 (2015) 924-936. (c) Upconverting nanoparticles: a versatile platform for wide-field two-photon microscopy and multi-modal *in vivo* imaging. Y. Park, K. T. Lee, Y. D. Suh, T. Hyeon, Chem. Soc. Rev. 44 (2015) 1302-17.

[107] Multi-Photon Excitation in Uncaging the Small Molecule Bioregulator Nitric Oxide. J. V. Garcia, F. Zhang, P. C. Ford, Philosophical Trans. Royal Soc. A., 371 (2013) 1995 20120129/1-20120129/25.

[108] Near-infrared–actuated devices for remotely controlled drug delivery. B.P. Timko, M. Arruebo, S.A. Shankarappa, J. B. McAlvin, O. S. Okonkwo, B. Mizrahi, C. F. Stefanescu, L. Gomez, J. Zhu, A. Zhu, J. Santamaria, R. Langer, D. S. Kohane PNAS (USA) 111 (2014) 1349-1354.

[109] Upconversion Assisted Near-Infrared (800 nm) Triggered Nitric Oxide Release from a new Cr(III) PhotoNORM. Photochemistry in Biocompatible Polymer Disks. P.-J. Huang, J. V. Garcia, A. Fenwick, G. Wu, A. D. DeMartino, P. C. Ford, manuscript in preparation.

[110] Light-controlled release of nitric oxide from solid polymer composite materials using visible and near infra-red light. J. D. Mase, A. O. Razgoniaev, M. K. Tschirhart, A. D. Ostrowski, PhotoChem. Photobiol. Sci. 14 (2015) 777-785.

[111] Core-shell materials bearing iron(II) carbonyl units and their CO-release via an upconversion process. J. Ou, W. Zheng, Z. Xiao, Y. Yan, X. Jiang, Y. Dou, R. Jiang, X. Liu, X. J. Mater. Chem. B, 5 (2017) 8161-8168.

[112] Remote-controlled delivery of CO via photoactive CO-releasing materials on a fiber optical device S. Glaeser, R. Mede, H. Goerls, S. Seupel, C. Bohlender, R. Wyrwa, S. Schirmer, S. Dochow, G. U. Reddy, J. Popp, M. Westerhausen, A. Schiller, Dalton Trans. 45 (2016) 13222-13233.

[113] Ruthenium nitrosyl grafted carbon dots as a fluorescence-trackable nanoplatform for visible light-controlled nitric oxide release and targeted intracellular delivery. Q. Deng, H.-J. Xiang, W.-W. Tang, L. An, S.-P. Yang, Q.-L. Zhang, J.-G. Liu, J. Inorg. Biochem. 165 (2016) 152-158.

[114] (a) Peptides as Targeting Elements and Tissue Penetration Devices for Nanoparticles. E. Ruoslahti, Adv. Materials, 24 (2012) 3747-3756. (b) Uptake and transfection efficiency of PEGylated cationic liposome–DNA complexes with and without RGD-tagging. R. N. Majzoub, C.-L. Chan, K. K. Ewert, B.F. B. Silva, K. S. Liang, E. L. Jacovetty, B. Carragher, C. S. Potter, C. R. Safinya, Biomaterials. 35 (2014) 4996–5005. (c) Targeted Intracellular Delivery of Proteins with Spatial and Temporal Control. D. P. Morales, G. Braun, A. Pallaoro, R. Chen, X. Huang, J. A. Zasadzinski, N. O. Reich, Molecular Pharmaceutics 12 (2015) 600-609.

[115] Fibrin-binding, peptide amphiphile micelles for targeting glioblastoma. E. J. Chung, Y. Cheng, R. Morshed, K. Nord, Y. Han, M. L. Wegscheid, B. Auffinger, D. A. Wainwright, M. S. Lesniak, M. V. Tirrell. Biomaterials 35 (2014) 1249-1256.

[116] (a) Ruthenium nitrosyl grafted carbon dots as a fluorescence-trackable nanoplatform for visible light-controlled nitric oxide release and targeted intracellular delivery. Q. Deng, H.-J. Xiang, W.-W. Tang, L. An, S.-P. Yang, Q.-L. Zhang, J.-G. Liu, J. Inorg. Biochem. 165 (2016) 152-158. (b) A multifunctional nanoplatform for lysosome targeted delivery of nitric oxide and photothermal therapy under 808 nm near-infrared light. H.-J. Xiang, M. Guo, L. An, S.-P. Yang, Q.-L. Zhang, J.-G. Liu, J. Mater. Chem. B 4 (2016) 4667-4674

[117] (a) Multi-functional Nanoparticles for Drug Delivery and Molecular Imaging, G. Bao, S. Mitragotri, S. Tong, Ann. Rev. Biomed Eng., 2013, 15:253-82. (b) Cell-mediated delivery of nanoparticles: Taking advantage of circulatory cells to target nanoparticles. A. C. Anselmo, S. Mitragotri, J. Controlled Release, 190 (2014) 531-541.

[118] Monocyte recruitment during infection and inflammation. C. Shi, E. G. Pamer, Nat Rev Immunol, 11 (2011) 762-74.

[119] Active Targeted Macrophage-mediated Delivery of Catalase to Affected Brain Regions in Models of Parkinson's Disease. Y. Zhao, M. J. Haney, V. Mahajan, B. C. Reiner, A. Dunaevsky, R. L. Mosley, A. V. Kabanov, H. E. Gendelman, E. V. Batrokova, J. Nanomed Nanotechnol, 54 (2011) S4.

[120] Mechanisms regulating the recruitment of macrophages into hypoxic areas of tumors and other ischemic tissues. C. Murdoch, A. Giannoudis, C. E. Lewis, Blood, 104 (2004) 2224-34.

[121] V. Balzani, P. Ceroni, A. Juris, “Photochemistry and Photophysics. Concepts, Research and Applications” Wiley-VCH Verlag Gmbh & Co. Weinheim, Germany 2014.

[122] Light Absorption in Photochemistry. H. Shaw, S. Toby, J. Chem. Educ. 43 (1966) 408-410.

[123] (a) Does a photochemical reaction have a reaction order? S. R. Logan, J. Chem. Educ. 74 (1997) 1304. (b) Does a Photochemical Reaction Have a Kinetic Order? S. Toby, J. Chem Educ. 82 (2005) 37.